

Optimization of the Throughput of a NOMA System

Balaji Kannappan Natarajan

A Thesis
in
The Department
of
Electrical and Computer Engineering

Presented in Partial Fulfillment of the Requirements
for the Degree of Master of Applied Science (Electrical Engineering) at
Concordia University
Montreal, Quebec, Canada

February 2021

© Balaji Kannappan Natarajan, 2021

**CONCORDIA UNIVERSITY
SCHOOL OF GRADUATE STUDIES**

This is to certify that the thesis prepared

By: Balaji Kannappan Natarajan

Entitled: Optimization of the Throughput of a NOMA System

and submitted in partial fulfillment of the requirements for the degree of

Master of Applied Science (Electrical and Computer Engineering)

complies with the regulations of this University and meets the accepted standards with respect to originality and quality.

Signed by the final examining committee:

_____	Chair
Dr. D. Qiu	
_____	External Examiner
Dr. C. Assi (CIISE)	
_____	Internal Examiner
Dr. D. Qiu	
_____	Supervisor
Dr. M.K. Mehmet Ali	

Approved by: _____
Dr. Y.R. Shayan, Chair
Department of Electrical and Computer Engineering

March 1, 2020

Dr. Mourad Debbabi, Interim Dean,
Gina Cody School of Engineering and
Computer Science

Abstract

Optimization of the Throughput of a NOMA System

Balaji Kannappan Natarajan

In an era of Internet of Things (IoT), new services are expected to generate heterogeneous traffic that involves both human-to-human and machine type communications (MTC). There will be MTC services that require massive connectivity, higher throughput, and low latency. 5G networks are under development to meet the needs of MTC. Non-Orthogonal Multiple Access (NOMA) has currently gained a traction in 5G for the realization of MTC. NOMA enables simultaneous utilization of resources by multiple users. This thesis considers Power Domain NOMA (PD-NOMA) among other variations for uplink communications. In PD-NOMA, users transmit signals simultaneously at pre-determined receive power levels. The base station decodes the signals using Successive Interference Cancellation (SIC) technique starting from highest power level. Each decoded signal is subtracted from the received signal to enable decoding of the next higher power signal. The decoding continues until a collision is detected at a power level. The signals at that power level as well as signals transmitted at the lower power levels cannot be decoded. The previous work on PD-NOMA assumed uniform user access to the system power levels. This thesis considers random non-uniform selection of power levels by the users.

The system model under consideration assumes that the new packets to be transmitted arrive according to a Poisson process and the time axis slotted. As a user may have only a single packet to be transmitted during any slot, each new packet is assumed to be generated by a different user. We consider two packet service strategies which are with and without packet loss.

In the packet loss service strategy, a packet can only be transmitted once, and packet is lost if that transmission is not successful. We determine the throughput of the system and then determine the optimal user access probabilities to the power levels that maximizes the throughput. We also determine the receive power levels for SIC as a function of the Signal-to-Interference-plus-Noise Ratio (SINR). Numerical results show that the optimal access probabilities are non-uniform, and they are a function of packet arrival rates. Further, in uniform access, the throughput

of the system drops to zero at higher power levels whereas, in optimal non-uniform choice, the system maintains a non-zero throughput. We also consider the case that the users may choose not to transmit their packets to reduce the collisions in the system. The packets that are not transmitted, are lost, however the system benefits from reduced collisions. Numerical results show that the optional transmission of packets achieves the same maximum throughput as compulsory packet transmission, but the throughput does not decrease with increasing packet arrival rate.

In the service strategy without packet loss, a user will keep transmitting a packet until it is successfully received by the base station. We derive the Probability Generating Function (PGF) of the distribution of the number of packets in the system at the steady-state by imbedding a homogenous Markov chain at the end of the slots. We determine enough number of equations to solve for the unknowns in the PGF. Then, we obtain the mean packet delay from the PGF of the number of packets in the system through application of the Little's result. Mean packet delay is a function of the user access probabilities to the power levels. We show how to determine the optimal access probabilities both for optional and non-optional transmission of a packet during a slot. We plot the mean packet delay as a function of the packet arrival rate for optimal user access probabilities both for optional and non-optional packet transmission, as well as for uniform choice of power levels. The numerical results show that the optimal access with optional transmission results in lowest mean packet delay and therefore in highest throughput.

Table of contents

List of Abbreviations	viii
List of Symbols	x
List of Figures	xi
1 Introduction and Literature Review.....	1
1.1 Overview	1
1.2 Realization of 5G through NOMA.....	1
1.3 Principle	2
1.4 Key Features.....	3
1.5 Advantages, Limitations, and Practical Considerations.....	4
1.5.1 Advantages.....	4
1.5.2 Limitations	4
1.6 Classification.....	5
1.7 Power-domain NOMA	6
1.7.1 Review and Analysis.....	9
1.7.2 Overview of a novel approach	12
1.8 Contribution of the thesis	13
1.9 Organization of the thesis.....	13
2 Modeling of a NOMA system with packet losses	15
2.1 Introduction	15
2.2 Mathematical model.....	15
2.3 System Modeling Case 1: A user will always transmit its packet	17
2.3.1 Throughput optimization	17
2.3.2 Determining received power levels for decoding.....	18

2.3.3	Numerical results	19
2.4	Case 2: A user may not always transmit its packet	25
2.4.1	Throughput Optimization.....	25
2.4.2	Numerical results	26
2.4.3	Determining received power for Level 1 decoding	28
2.5	Conclusion.....	30
3	Modeling of a NOMA system without packet losses	31
3.1	Introduction	31
3.2	Mathematical model.....	31
3.2.1	Derivation of the PGF of the number of packets in the system	33
3.2.2	Application of homogeneous Markov chain analysis.....	35
3.2.3	Average mean packet delay	36
3.2.4	User access probabilities.....	37
3.3	Methods of determining user access probabilities	39
3.3.1	Optimal User access probabilities with non-optional transmit.....	39
3.3.1.1	Analysis	39
3.3.1.2	Numerical results and Discussion.....	39
3.3.2	Optimal user access probabilities with optional transmit	47
3.3.2.1	Analysis	47
3.3.2.2	Numerical results and Discussion.....	48
3.3.3	Uniform user access probabilities with non-optional transmit	56
3.3.3.1	Analysis	56
3.3.3.2	Numerical results and Discussion.....	57
3.3.4	Numerical results for the mean packet delay	61
3.4	Conclusion.....	63

4	Conclusion and Future Work.....	64
	References.....	66

List of Abbreviations

Abbreviation	Definition
IoT	Internet of Things
MTC	Machine-Type Communications
1G	First Generation
2G	Second Generation
3G	Third generation
4G	Fourth Generation
5G	Fifth Generation
OMA	Orthogonal Multiple Access
NOMA	Non-Orthogonal Multiple Access
TDMA	Time Division Multiple Access
OFDMA	Orthogonal Frequency Division Multiple Access
BS	Base Station
CSI	Channel State Information
PDMA	Power Domain Multiple Access
EE-SC	Energy Efficiency-Spectral Efficiency
SINR	Signal-to-Interference-plus-Noise-Ratio
CDMA	Code Domain Multiple Access
SIC	Successive Interference Cancellation
AUD	Active User detection
CE	Channel Estimation
CS	Compressive Sensing
MIMO	Multiple-Input-Multiple-Output
CD-NOMA	Code Domain NOMA
PD-NOMA	Power Domain NOMA
LDS	Low Density Spreading
SDR	Software Defined Radio

IDMA	Interleave Division Multiple Access
BDM	Bit Division Multiplexing
SDMA	Spatial Division Multiple Access
PDMA	Pattern Division Multiple Access
MUSA	Multi-User Shared Access
NM-ALOHA	NOMA with slotted ALOHA
CRRD	Contention Resolution Repetition Diversity
IRSA	Irregular Repetition Slotted ALOHA
PGF	Probability Generating Function

List of Symbols

Variable	Definition
L_i	Received power at power level i
N	Number of Power Levels
λ	Arrival rate in a system
P_k	Probability that k users will have a packet to transmit during a slot
ϕ_i	SINR at power level i
γ	SINR threshold
p_i	Optimal access probabilities to a power level i
M	maximum number of packets for which success probability is not constant.
I_i	Number of packets successfully transmitted at slot i
q_{kj}	Prob (j packets being transmitted successfully during a slot given that there were k packets at the beginning of a slot)
q_j	Prob (j packets being transmitted successfully during a slot)
$Q_i(z)$	PGF of the distribution of the number of packets in the system at the end of i^{th} slot
$Q(z)$	PGF of the distribution of the number of packets in the system at steady state
\bar{n}	Average number of users in the system
\bar{d}	mean packet delay
\vec{k}	vector of the number of users choosing each power level

List of Figures

Fig. 1.1 Classification of multiple access technologies

Fig. 1.2 Principle of Power-Domain NOMA

Fig. 2.1. Throughput as a function of probability that a user chooses power level L_1 for $N=2$ power levels with arrival rate as a parameter

Fig. 2.2. Optimal access probabilities to a power level, p_i , as a function of the traffic arrival rate for $N = 2$ power levels

Fig. 2.3. Throughput as a function of packet arrival rate for optimal and uniform access probabilities to a power level for $N = 2$ power levels

Fig. 2.4. Optimal access probabilities to a power level, p_i , as a function of the traffic arrival rate for $N = 3$ power levels

Fig. 2.5. Throughput as a function of packet arrival rate for optimal and uniform access probabilities to a power level for $N = 3$ power levels

Fig. 2.6. Optimal access probabilities to a power level, p_i , as a function of the traffic arrival rate for $N = 4$ power levels

Fig. 2.7. Throughput as a function of packet arrival rate for optimal and uniform access probabilities to a power level for $N = 4$ power levels

Fig. 2.8. Optimal access probabilities to a power level, p_i , as a function of the traffic arrival rate for $N = 5$ power levels

Fig. 2.9. Throughput as a function of packet arrival rate for optimal and uniform access probabilities to a power level for $N = 5$ power levels

Fig. 2.10. Optimal access probabilities as a function of the packet arrival rate for $N = 2$ power levels power levels

Fig. 2.11. Optimal access probabilities as a function of packet arrival rate for $N = 4$ power levels

Fig. 2.12. Optimal access probabilities as a function of packet arrival rate for $N = 6$ power levels

Fig. 2.13. Throughput as a function of the packet arrival rate for $N=2, 3, 4$ and 6 power levels

Fig. 2.14. Received power level L_1 as a function of the packet arrival rate for $N=4$ power levels with threshold SINR as a parameter

Fig. 2.15. Received power at power level L_1 as a function of the number of power levels for fixed value of SINR, $\gamma = 3$ and packet arrival rate as a parameter

Fig. 2.16. Average received power level L_1 as a function of the packet arrival rate for $N=4$ power levels with threshold SINR as a parameter

Fig. 3.1. Optimal access probabilities as a function of the number of packets in the system for $N=2$ power levels

Fig. 3.2. Success probabilities as a function of number of packets for $N=2$ power levels

Fig. 3.3. Throughput as a function of the packet arrival rate for $N=2$ power levels

Fig. 3.4. Optimal access probabilities as a function of the number of packets in the system for $N=3$ power levels

Fig. 3.5. Success probabilities as a function of number of packets for $N=3$ power levels

Fig. 3.6. Throughput as a function of the packet arrival rate for $N=3$ power levels

Fig. 3.7. Optimal access probabilities as a function of the number of packets in the system for $N=4$ power levels

Fig. 3.8. Success probabilities as a function of number of packets for $N=4$ power levels

Fig. 3.9. Throughput as a function of the packet arrival rate for $N=4$ power levels

Fig. 3.10. Optimal access probabilities as a function of the number of packets in the system for $N=5$ power levels

Fig. 3.11. Success probabilities as a function of number of packets for $N=5$ power levels

Fig. 3.12. Throughput as a function of the packet arrival rate for $N=5$ power levels

Fig. 3.13. Optimal access probabilities as a function of the number of packets in the system for $N=2$ power levels

Fig. 3.14. Success probabilities as a function of number of packets for $N=2$ power levels

Fig. 3.15. Throughput as a function of the packet arrival rate for $N=2$ power levels

Fig. 3.16. Optimal access probabilities as a function of the number of packets in the system for $N=3$ power levels

Fig. 3.17. Success probabilities as a function of number of packets for $N=3$ power levels

Fig. 3.18. Throughput as a function of the packet arrival rate for $N=3$ power levels

Fig. 3.19. Optimal access probabilities as a function of the number of packets in the system for $N=4$ power levels

Fig. 3.20. Success probabilities as a function of number of packets for $N=4$ power levels

Fig. 3.21. Throughput as a function of the packet arrival rate for $N=4$ power levels

Fig. 3.22. Optimal access probabilities as a function of the number of packets in the system for $N=5$ power levels

Fig. 3.23. Success probabilities as a function of number of packets for $N=5$ power levels

Fig. 3.24. Throughput as a function of the packet arrival rate for $N=5$ power levels

Fig. 3.25. Success probabilities as a function of number of packets for $N=2$ power levels

Fig. 3.26. Throughput as a function of the packet arrival rate for $N=2$ power levels

Fig. 3.27. Success probabilities as a function of number of packets for $N=3$ power levels

Fig. 3.28. Throughput as a function of the packet arrival rate for $N=3$ power levels

Fig. 3.29. Success probabilities as a function of number of packets for $N=4$ power levels

Fig. 3.30. Throughput as a function of the packet arrival rate for $N=4$ power levels

Fig. 3.31. Success probabilities as a function of number of packets for $N=5$ power levels

Fig. 3.32. Throughput as a function of the packet arrival rate for $N=5$ power levels

Fig. 3.33. Average packet delay as a function of the packet arrival rate for $N=2$ power levels

Fig. 3.34. Average packet delay as a function of the packet arrival rate for $N=3$ power levels

Fig. 3.35. Average packet delay as a function of the packet arrival rate for $N=4$ power levels

Fig. 3.36. Comparison of Success probabilities as a function of number of packets for $N=2$ power levels

Fig. 3.37. Comparison of Throughput as a function of the packet arrival rate for $N=2$ power levels

Fig. 3.38. Average packet delay as a function of the packet arrival rate for number of power levels $N=2$ power levels

Fig. 3.39. Success probabilities as a function of number of packets for $N=4$ power levels

Fig. 3.40. Comparison of Throughput as a function of the packet arrival rate for $N=4$ power levels

Fig. 3.41. Average packet delay as a function of the packet arrival rate for number of power levels $N=4$ power levels

Fig. 3.42. Comparison of success probabilities as a function of number of packets for $N=2$ power levels

Fig. 3.43. Comparison of throughput as a function of the packet arrival rate for $N=2$ power levels

Fig. 3.44. Average packet delay as a function of the packet arrival rate for number of power levels $N=2$ power levels

Fig. 3.45. Success probabilities as a function of number of packets for $N=4$ power levels

Fig. 3.46. Comparison of throughput as a function of the packet arrival rate for $N=4$ power levels

Fig. 3.47. Average packet delay as a function of the packet arrival rate for number of power levels $N=4$ power levels

Chapter 1

Introduction and Literature Review

1.1 Overview

In an era of Internet of Things (IoT), there is a swift increase in the mobile traffic and a demand for massive connectivity in Machine-Type Communication (MTC). Hundreds and thousands of machine-type devices are already connected in the 4G cellular network, and this number is said to increase exponentially in the near future[1][2]. As opposed to the conventional 3.9 and 4G transmissions, this dramatic increase necessitates the Future Radio Access schemes to meet the standards of improved efficiency, with lower latency, especially when the system is employed in a delay-sensitive environment like medical and tactical communications. It also necessitates a crucial uplift in performance gain of the system, due to ever-growing and massive user traffic.

5G networks is a novel topic of interest to the researchers, to meet such demands of new cellular communication services. These services generate heterogeneous traffic and involves both human-to-human and MTC. These services may demand higher throughput, lower latency, and massive connectivity [1].

1.2 Realization of 5G through NOMA

The communication devices of the past decades allocated the user resources, namely, frequency, time, and code, in feasible ways, to develop wireless communication models viz., 1G, 2G, 3G and 4G. These design principles were categorized as Orthogonal Multiple Access (OMA), as resources were allocated orthogonally among the users. Although OMA systems had low-complexity cost-efficient receivers, they faced a backlog in serving large number of user devices and the principle of orthogonality of resource allocation became futile due to channel-inherent losses, like co-channel interference[3]. Furthermore, an increasing demand of resources adversely affects the system performance metrics like sum-rate, throughput, outage probability and bit error rate. Thus, 5G networks which is expected to support massive number of devices that generates sporadic MTC traffic, may be better served through Non-Orthogonal Multiple Access (NOMA).

1.3 Principle

The main principle behind NOMA is to share a single resource block with more than one user device in the same resource. In contrast to OMA, NOMA can simultaneously serve multiple number of users using a single orthogonal resource block, which may be a frequency channel, a spreading code or time slot etc. On the other hand, OMA techniques such as, time-division multiple access (TDMA) or orthogonal frequency division multiple access (OFDMA), may only serve a single user in each orthogonal resource block at any time.

In order to serve more than one user in the same wireless resource block in the downlink, linear superposition of information signals is carried out at the Base Station (BS) while achieving multiple access, either in power domain or code domain. Decoding of these superposed signals at the receiver, requires subtraction of all unrelated signals and noise, referred as Inter-User Interference, until the receiver finds its intended signal [4][5][6]. Thus, careful allocation of power to the users is imperative to ensure user fairness [7] and avoid intra-cell interference [8]. Though this approach increases the receiver complexity, it lets the system to handle large number of users to be supported over the same resource block.

NOMA is often suitable for downlink transmissions owing to the fact that NOMA allocates the power to the users whose Channel State Information (CSI) is known [9]. Thus, we need the CSI to be synchronized throughout the system, which can be attained by employing coordinated access system such as a scheduler [10][11]. As per the works of Kumar et al., [33], it is quite evident that NOMA provides better Energy Efficiency-Spectral Efficiency (EE-SE) Tradeoff compared to the conventional OMA methods. Spectral Efficiency, as defined by Kumar et al., [33] is nothing but the ratio of maximum sum capacity to the bandwidth of the system. Hence, even though uncoordinated access systems provide better throughput and lower signaling overhead [9], it cannot be employed to an uplink transmission system due to lack of CSI [12][13]. A model with a set of pre-determined power levels for allocating to the users in the resource block as discussed Choi in [9] is a way to mitigate this problem.

Throughput optimization is accomplished with a Power Domain Multiple Access (PDMA) scheme using non-coordinated transmission [9] or based on rate optimization and fixed target Signal-to-Interference-plus-Noise-Ratio (SINR) [14]. It is to be noted that, due to widespread requirement of low complexity systems which are matched to sporadic traffic of large number of

users, current models as proposed in some literature works assume a power level selection by the user based on a uniform distribution [7][9][14][26].

1.4 Key Features

Although NOMA is perceived to be quite similar to Code-Division Multiple Access (CDMA) that is used in 3G systems, they have a striking difference in the model principle. While CDMA users are provided multiple access through spreading codes, NOMA utilizes user-specific spreading sequences that are non-orthogonal and have a low correlation coefficient [15][16]. Some of such features that make NOMA a promising candidate for 5G systems, are:

Non-orthogonality:

The crucial reason for the usage of NOMA in 5G and Future Radio Access (FRA) systems solely owes to the fact that the bottleneck of an ever-increasing demand can be mitigated by use of non-orthogonal signals. Thus, multi-user multiplexing is achieved in a completely different dimension, rather than time, frequency, or code.

Superposition coding:

The utilization of superposition coding in the transmission systems has been into usage since the infancy of 3G systems. But superposition coding in combination with power domain multiplexing, which is realized in NOMA, allows the transmitter to transmit information signals of multiple users in a superposed fashion [17][18].

Successive Interference Cancellation :

The basic principle behind Successive Interference Cancellation (SIC) is that , when SIC is applied, the information signal of any user is decoded, by treating the other unrelated signals as interference and noise. This allows the receiver to decode single user signal, thus reducing the system complexity. This enables the NOMA system to mitigate intra-cell interference and improve cell-edge throughput. Joint Decoding is another well-known decoding technique used for uplink NOMA.

Message passing algorithm:

This can be conceptualized as an iterative decoding algorithm that has been used since the growth of information theory in communication. Usage of several types of message passing algorithms in NOMA systems enables us to recover the CSI vector for channel feedback and mitigate the problems of Active User Detection (AUD) and Channel Estimation (CE)[19][20].

1.5 Advantages, Limitations, and Practical Considerations

1.5.1 Advantages

- NOMA found its attention and edge due to its compatibility. Various research and literature works have shown that NOMA can be incorporated with other OMA techniques [21][22][23].
- NOMA technique allows the transmission and reception system to support massive Machine-Type Communications (mMTC).
- Superior EE-SE tradeoff [33] and drastic improvement in cell-edge throughput.
- Feedback mechanism requires only received channel strength and it does not require complete CSI during each iteration, thus making the feedback more relaxed and flexible.
- Realization of semi-grant and grant-free NOMA [24] with blind detection and Compressive Sensing (CS) techniques [25] is an important feature supported by FRA since it reduces the latency and the signaling overhead.

1.5.2 Limitations

Although NOMA has its own recognition in 5G environment, NOMA is still under development and it is still in its infancy stage. Some of the limitations are:

- For grant-free transmission, the number of users admitted to the same channel is not capped, which can lead to a failure of multi-user detection.
- Power-domain NOMA requires the users to have a considerable amount of difference in channel gain, so that they can be manipulated into multi-user multiplexing. This is because, the channel gain difference is essentially utilized for Transmit Power Allocation (TPA) in superposing at the transmitter side. The information signals of users with similar channel gains will lead to co-channel interference and the receiver will take longer time to decode

the signal, thus increasing the transmission time. This requires a system design incorporating clustering algorithm.

- An erroneous decoding of a signal in the higher transmission power level, will lead to an obliteration of all the other signals beneath it.
- A joint optimization of rank and transmission power assignment is required in case of Multiple-Input-Multiple-Output (MIMO) NOMA in order to enhance the performance of multi-user power allocation.
- It becomes challenging to realize NOMA in uplink channel, without proper mechanism of CSI feedback.

Other limitations in practical deployment like Multi-user power allocation, signaling overhead, SIC error propagation, high mobility performance and MIMO combination, have also been discussed by Benjebbour et al [6].

1.6 Classification

Although there have been many researches in realizing NOMA in different dimensions, the most commonly studied categories fall under two brackets: code domain NOMA, CD-NOMA, and power domain NOMA, PD-NOMA, where the former obtains spreading gain at the cost of more bandwidth, while the latter assigns distinct power levels to users to obtain better performance. Classification of multiple access technologies is shown in Fig. 1.1.

There have been improvisations on the aforementioned categories, like the technique that applies Low Density Spreading (LDS-CDMA), which is further realized as Sparse Code Multiple access and SIC Amenable Multiple Access. Other closely related multiple access schemes that also benefit Software Defined Radio (SDR-MA), are Interleave Division Multiple Access (IDMA), Bit Division Multiplexing (BDM), Spatial Division Multiple Access (SDMA), Pattern Division Multiple Access (PDMA) and Multi-User Shared Access (MUSA).

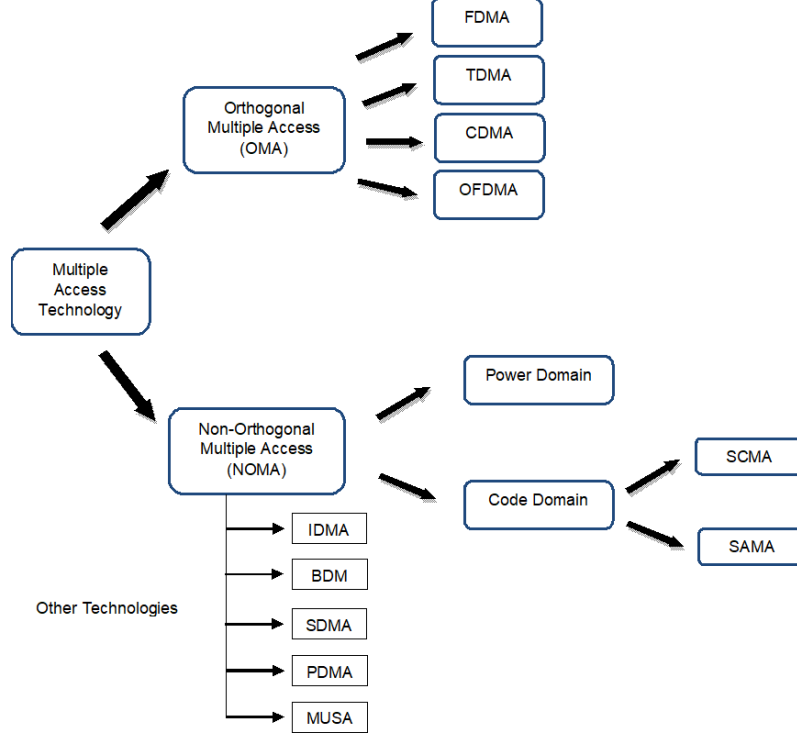


Fig. 1.1 Classification of multiple access technologies

It is to be noted that most of the literature works and researches focus on Power Domain-NOMA. Initially, NOMA has been considered for downlink transmissions from base stations to the users since it requires coordination and channel state information (CSI). However, as mentioned earlier, NOMA has also been proposed to be used in uplink transmissions, from users to base stations, in random access channels without coordination by the base station [9].

1.7 Power-domain NOMA

In a typical downlink NOMA model, the transmitted signal is nothing but the superposed signal from each of the UE in the system. More power is allotted to the farthest user to cope up with the transmission losses. Thus, the transmitted signal $x(t)$ may be represented as,

$$x(t) = \sum_{k=1}^K \sqrt{\alpha_k P_T} x_k(t)$$

Where, α_k is the power allocation co-efficient, P_T is the total transmit power and $x_k(t)$ is the individual information signal of UE_k. The received signal $y_k(t)$ may be written as,

$$y_k(t) = x(t)h_k(t) + w_k(t)$$

Where $h_k(t)$ is the channel coefficient between the BS and UE_k, and $w_k(t)$ is the additive white noise. SIC is implemented at the UE side, where the optimal order of decoding is in the decreasing order of channel gain. In other words, the first signal to be decoded is the strongest signal in $y_k(t)$. This decoded component is amplified in accordance with the power allocation co-efficient and re-encoded, so that it can be subtracted from the recent composite signal. This process is successively repeated, until the information signal of user k, $x_k(t)$ is extracted. Thus, assuming ideal conditions of successful decoding and zero error propagation, any user k , may extract its signal from the composite received signal by successfully eliminating the user signals $x_K, x_{K-1} \dots x_{k+1}$. The signals $x_{k-1}, x_{k-2}, \dots, x_1$ are simply considered as interference.

Thus, the channel capacity of any user k may be defined as,

$$R_k = W \log_2 \left(1 + \frac{P_k |h_k|^2}{w_k + \sum_{j=1}^{k-1} P_j |h_j|^2} \right)$$

A simplified model with one BS and 2 UE's is illustrated in fig. 2. This model can be conveniently adopted towards an uplink transmission with the BS being the receiver. Thus, the terms, User Equipment and BS may be interpreted interchangeably. UE-2 being the farthest, is allotted more transmit power in the system. At UE-2, there is no signal cancellation involved, as $x_2(t)$ is the first to be decoded. $x_1(t)$ is considered as interference signal. At UE-1, $x_2(t)$ is decoded and subtracted from y_1 so that $x_1(t)$ can be decoded without any interference from $x_2(t)$.

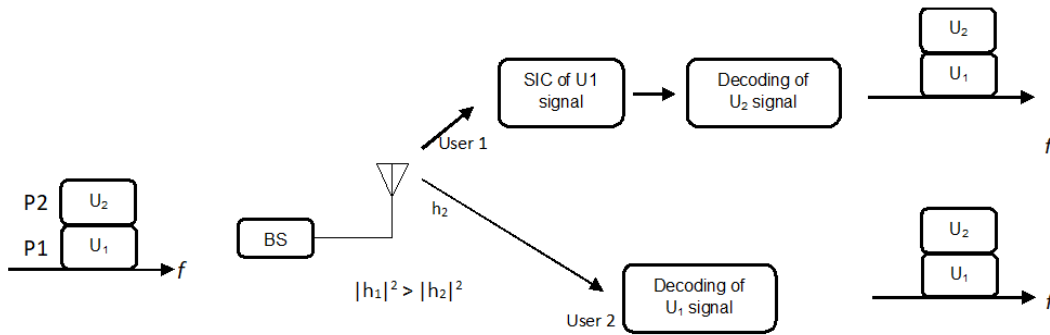


Fig. 1.2 Principle of Power-Domain NOMA

Here, NOMA is utilized to simultaneously serve multiple users in the same resource domain (time, frequency, code or OFD resource block), by fairly splitting them in the power domain. This lets the user signal to be superposed with other signals during transmission, thus achieving non-orthogonality. Though employing PD-NOMA has its own advantages, many factors have to be considered in practical implementation, as mentioned earlier, including user fairness, delay in critical message delivery, and choice of coordinated or uncoordinated system based on the requirement.

It is highly crucial to take care of optimal power allocation to the users since the resource is limited. The system may utilize either coordinated power level system or random-access system. As discussed by Park *et al.*, [7], application of either methods, completely depends on the type of system needed for the problem considered. That being said, it is observed from the studies of Park *et al.*, [7], that usage of coordinated access systems provides CSI feedback and is mostly used in downlink channels. But this comes at a cost of higher scheduling delay and signaling overhead which reduces the performance. Usage of uncoordinated access, such as the access mechanisms that use contention protocols rather than reservation protocols, provides improved spectral efficiency in relation to that of coordinated systems, but the backlog of this method is that, TPA is required in user multiplexing to mitigate inter-user interference and achieve maximum sum rate. Since uncoordinated access is contention based, rather than reservation based, there is high probability that there will be collision of packets if two or more users transmit with same transmit power, causing unsuccessful transmission. This relatively degrades the throughput. Moreover, without the availability of CSI in the system, it is difficult to implement uncoordinated access in uplink channel.

We consider a PD-NOMA model with single channel slotted ALOHA as per some literature works in [7][9][14][26]. It is also assumed that the system is fully aware of the CSI of the users contending. The basic approach used in this thesis, in regard to PD-NOMA can be listed as follows:

- A hierarchical power level structure is considered for the transmission system, with adequate power difference between each level, to avoid co-channel interference. It is to be noted that the system has decreasing order of power levels.
- A random-access channel is considered. Here we utilize slotted ALOHA NOMA channel, as per most of the works by Choi et al [9][14][26].

- Complete knowledge of CSI is assumed. We also consider a set of pre-determined power levels in order to incorporate into an uplink channel.

1.7.1 Review and Analysis

In this section, I review the mathematical models and corresponding results of the works pertaining to that of this thesis under study.

The previous works of Choi have been predominantly considered in this thesis[9]. Choi considers a multichannel NOMA with slotted ALOHA scheme, applied in uplink channel. A set of predetermined power levels have been considered. Throughout the paper, a single cell with one BS and multiple users with multiple orthogonal subchannels are considered. The users choose from one of the B subchannels based on a uniform distribution. It is also observed that a user chooses one of the power levels with equal probability according to the uniform distribution.

This research by Choi [9] also assumes complete awareness of CSI. In fact, a beacon signal is used to synchronize the estimation of CSI. However, channel impairment metrics like fading, are ignored in this paper, and left for future study.

When an active user k , randomly chooses a power level v_l from the hierarchy $v_1 > v_2 > \dots > v_l > \dots > v_L > 0$, where L is the number of power levels, then the transmission power of user k is defined to be,

$$P_k = \frac{v_l}{\alpha_k} \quad (1.1)$$

Where α_k is the channel power gain from user k to the BS. It is given by $\alpha_k = |h_k|^2$.

If Γ is the target SINR of the system, then, the transmit power of each level is determined by,

$$v_l = \Gamma(\Gamma + 1)^{L-1} \quad (1.2)$$

Choi has also suggested that the decoding of all the superposed signals may be successful only if the number of active users is less than or equal to the number of power levels, failing which, there may be data loss due to collision, which indeed, is the basic principle behind slotted ALOHA.

It is shown that higher throughput can be attained as L increases, while being mindful about the exponential increase in the value of v_l as L increases. The increase in the transmission power

is mitigated through channel dependent Energy Efficient selection. This is illustrated through a two-layer model. Assuming that the users are uniformly distributed within the cell range, they can be divided into two groups in order to access the two different layers, where the system is mindful about the channel gains and path losses.

Choi also applies the basic PD-NOMA model to a multichannel ALOHA and it is observed from the numerical results that the throughput of NOMA-ALOHA increases as a function of L , without any bandwidth expansion.

Simulation results and studies have been performed with regard to the average transmission power with and without channel dependent power level (or subchannel) selection scheme. It is proven in the literature that the average transmission power of any user is much lower when channel dependent selection scheme is implemented in NOMA-ALOHA [9].

While a fully aware CSI model is assumed in [9], [14] deals with a slightly modified system. The key difference of this paper from the previous one, is that a NOMA based Slotted ALOHA model which exploits the power difference, is studied, and a closed-form expression for maximization of throughput is derived by utilizing optimal transmission rates in each layer. Application of multiple individual 1-dimensional optimization of transmission rates, is consequently inferred. At receiver side, SIC implemented and a brief emphasis on Contention Resolution Repetition Diversity (CRRD) with delay constraint is performed. A graphical Analysis of Irregular Repetition Slotted ALOHA (IRSA) is also performed, based on the works of Liva *et al.*, and Paolini *et al* [27][28][29]. This paper does not assume fully aware CSI, rather, the success of SIC depends on the packet collision and instantaneous CSI.

Though power allocation, rate allocation and arrival rate control are the key metrics for throughput maximization, this paper [14] focuses only on rate optimization to maximize throughput. Assumption of multi power level, multi-channel, and multi-user environment with uniform selection of power levels and subchannels, is similar to the previous works of Choi [9]. Layered random access model considers that the signal power of any user choosing layer l must be set to P_l and the number of bits per channel must be set to R_l . Signal decoding at the receiver side is performed with SIC. It is to be noted that, the receiver stops the SIC if there is a packet collision or if SIC fails to decode a signal. Thus, all the data, that is sent by the power levels below the hierarchy is lost.

One of the key assumptions in this paper [14] is that all the users choose a power level randomly, as the users have same average channel power gains in contrast to what is being considered by Liang *et al.*, and Wang *et al* [30][31]. The author also compares the above proposed model with the IRSA scheme that is explicated in [34]. A simplified model with fixed target SINR is considered for comparison, for homogeneity in assumptions.

In order to increase the maximum throughput, the concept of Contention Resolution Repetition Diversity (CRRD) is discussed [14]. The aforementioned layered NOMA is modified in such a way that the system transmits multiple copies of the same packet (referred as bursts) at random time. It is to be noted that the burst packet also comprises the information of the slot to which it belongs, in order to facilitate the removal of replicas [35].

In order to contemplate the purpose of coordinated or uncoordinated systems in 5G, a complete study of the work by Park *et al.*, [7] is necessitated. The major objective of this research [7] is to treat critical messages with higher priority and allocate power level accordingly. Park utilizes the notion of power level partitioning to achieve this. As discussed earlier, usage of coordinated systems increases user fairness, and cell-edge throughput. Keeping the system always synchronized with the CSI lets the system to perform better with lower receiver complexities. However, it increases the signaling overhead and scheduling delay, thus, making it unfit for transmission of critical messages. On the other hand, usage of non-coordinated systems like ALOHA channel, increases the spectral efficiency with a relatively better latency. Coordination in transmission is achieved either by using beacon signal [9] for CSI estimation, or exploiting the different time of arrivals [30]. But the downside of non-coordinated systems is that the throughput is degraded due to duplicate selection of power levels [7].

Thus, Park suggests a proposal of hybrid power level allocation, that supports an optimal transmission of both critical and non-critical messages. A study has been performed in modelling of optimal message-aware uplink transmit power level partitioning that maximizes the throughput of non-critical messages, while maintaining a threshold throughput for critical messages [7].

Considering the total number of power levels to be l , they partitioned into two groups in this model: l_p power levels for non-critical messages and $l_c = l - l_p$ for critical messages. The model proposes to use the top l_p power levels with coordinated transmissions for non-critical

messages, and the bottom l_c power levels for critical messages that uses non-coordinated transmissions. Since the duplication is possible for critical message transmission, the model should support enough number of l_c power levels to satisfy the reliability constraint. Thus, the objective of this paper is considered to be maintaining the transmission success probability just sufficient for the reliability constraint, so that the overall throughput is minimally affected. It is to be noted that, the model uses uniform selection of power levels.

One of the challenges that is discussed in [7] is that the BS is unable to know the exact number of devices having critical messages. This is mitigated by minimizing the mean-squared error and estimating the failures that happen due to collisions. Simulation results have also been discussed which shows evident increase in success probability of high-priority messages as a function of target reliability.

1.7.2 Overview of a novel approach

Although there have been several schemes developed and pioneering works have been investigated to mitigate collisions in random access NOMA, the concern of retransmission latencies and deterioration in sum rate of the system seems to be inevitable. Moreover, there are very few literature works that focus on the contention dynamics during re-transmission or collision. One of the crucial modifications to the aforementioned works is that this thesis deals with the adoption of imbedded Markov chain at random spaced points to develop a lossless model. In this thesis, we consider a single channel slotted NOMA ALOHA model that uses PD-NOMA in uplink transmissions, between users and a BS. Our work has a key difference from the other models, that we employ a non-uniform choice of power-levels that maximizes the throughput. We also allow an active user the choice of transmitting or not transmitting during a slot, which further improves the throughput under heavy traffic. The proposed model readily extends to a system with multiple channels where a user chooses a channel for its transmission randomly. Throughout the thesis, we assume that the users are fully aware of their CSI which means that the system adapts to the varying channel properties and manages the combined effects of channel gains and fading coefficients.

1.8 Contribution of the thesis

As aforementioned, this thesis deals with a single channel slotted PD-NOMA model, with non-uniform power level selection and CSI-aware multiple users. Following are the contributions made by this thesis:

- The NOMA-ALOHA model is analyzed based on two service strategies, namely, with and without packet losses. Under packet losses category, a packet has only a single transmission attempt, if this attempt is not successful, then that packet is lost. In lossless model, collided packets remain in the system and retransmission attempts of a packet are continued until the packet transmission is successful.
- Under packet loss model, the access probabilities of the layers (power levels) have been mapped to a function that is constraint upon maximal throughput, thus optimizing the system to achieve higher efficiency. The analysis of results is twofold: throughput study under non-optional transmission and optional transmission.
- The service category of lossless model takes retransmission into account, and utilizes imbedded Markov chain analysis, and state transition analysis for the solution of the optimization problem.
- The numerical results of the lossless model are investigated under three different access methods to the power levels, optimal access with nonoptional transmission, optimal access with optional transmission and uniform access with nonoptional transmission.
- Mean packet delay of the system is determined from the PGF of the number of packets in the system through application of the Little's result and discussed briefly.

1.9 Organization of the thesis

The remainder of the thesis is organized as follows:

Chapter 2 deals with a system model with packet loss. Throughput optimization is performed for two cases: non-optional user transmission and optional user transmission. The required received signal power is determined and results are investigated. Numerical results are discussed in final section.

Chapter 3 proposes a mathematical model without packet losses. System design is performed mathematically by Imbedded Markov chain analysis, state transition analysis with homogeneous

Markov chain, and throughput optimization with user access probabilities as variables. Numerical results are presented under three subcategories: non-optional user transmission, optional user transmission and uniform access. Chapter 4 concludes the thesis with final remarks.

Chapter 2

Modeling of a NOMA system with packet losses

2.1 Introduction

In this study, we consider a single channel conventional PD-NOMA scheme [1][4]. We assume that each user may only have a single packet to transmit at any time. The users choose a power level randomly and transmit their packets synchronously. The packets that cannot be decoded by the receiver are lost. The optimal power level choice that maximizes throughput of the system is determined and compared with uniform choice of power levels under two cases. In one case, a user always has to transmit its packet and in the other case it may choose not to transmit its packet. The required received power levels for decoding at the receiver are also determined.

2.2 Mathematical model

We assume that there are N power levels denoted by $L_1, L_2, \dots, L_i, \dots, L_N$ where L_i denotes the received power at level i at the BS. We assume that the received signal at level i has higher power than the signal at level $i+1$, $L_i > L_{i+1}$. The time-axis is slotted, and the transmission time of a packet takes a single slot. It is assumed that a user chooses to transmit its packet at power level L_i with probability p_i during a slot. We will refer to p_i as access probability, $i = 1 \dots N$. We assume that each user may have a single packet to transmit during a slot, therefore the number of users with packets and total number of packets to be transmitted during a slot are same and they will be used interchangeably. We assume that the number of users with packets to transmit during a slot is given by a Poisson distribution with parameter λ packets/slot.

It is noted that a collision occurs if two or more users choose to transmit their packets at the same power level [3]. The transmission of a packet will be successful if the packet can be decoded by the receiver. The receiver will be able to decode a packet transmitted at power level L_i , if no collisions occur at power levels L_1 to L_i and Signal-to-Interference-plus-Noise-Ratio (SINR) is

above a threshold. Those packets that could not be successfully transmitted during a slot are lost. The BS will receive the superposition of all the signals transmitted by all the users plus background noise. The successive interference cancellation (SIC) technique is used to decode the signals. The BS starts decoding packets from highest towards the lowest power level. When a packet is decoded successfully, then its signal is removed from the received signal. Then, the receiver starts decoding the packet transmitted at the next power level. This decoding process continues until there is a collision at a power level. The packets at that and subsequent power levels cannot be decoded.

Let us make the following definitions,

$P_k = \text{Prob} (k \text{ users will have packets to transmit during a slot})$

$P_{ki} = \text{Prob} (k \text{ users will choose to transmit at power level } L_i)$

$P_{Ci} = \text{Prob} (\text{a collision will occur at power level } L_i)$

$P_{Q_n} = \text{Prob} (\text{the first collision occurs at power level } L_n).$

U : total number of packets decoded successfully during a slot.

$$I_j = \begin{cases} 1 & \text{if a packet is transmitted successfully at} \\ & \text{power level } L_j \\ 0 & \text{otherwise} \end{cases}$$

The system will be designed in a way that access probabilities will be optimized such that throughput in each slot will be maximized. This will be main difference of our algorithm than what is being used in the literature. Throughout this work, as considered in [3], we assume that the user is aware of its CSI.

In the following sections throughput of the system is derived as a function of the user access probabilities to the power levels. Then, the optimal access probabilities that maximize the system throughput are determined. In the following, the throughput of the system is optimized for two cases, in first case, user with a packet will always transmit its packet in the next slot and in the other case, the user may choose to transmit or not to transmit its packet during the next slot.

2.3 System Modeling Case 1: A user will always transmit its packet

In this case, a user will always transmit its packet at one of the power levels. We will present the throughput optimization, determine the power levels required for decoding and present some numerical results.

2.3.1 Throughput optimization

From the definitions in the previous section, we have the following results. Since the number of users with packets to transmit during a slot is given by the Poisson distribution [32],

$$P_k = \frac{e^{-\lambda} \lambda^k}{k!}, \quad k = 0, 1, 2, \dots \quad (3.1)$$

Since each user chooses to transmit at power level L_i with probability p_i ,

$$P_{ki} = \frac{e^{-\lambda p_i} (\lambda p_i)^k}{k!}, \quad k = 0, 1, 2, \dots \quad (3.2)$$

$$P_{Ci} = 1 - \text{Prob}(0 \text{ or } 1 \text{ user transmitting at power level } L_i)$$

From (3.2),

$$P_{Ci} = 1 - P_{0i} - P_{1i} = 1 - e^{-\lambda p_i} - \lambda p_i e^{-\lambda p_i} \quad (3.3)$$

$$P_{Q_n} = P_{Cn} \prod_{i=1}^{n-1} (1 - P_{Ci}), \quad n > 1. \quad (3.4)$$

We note that for $n = 1$ the number of power level becomes one and thus,

$$P_{Q_n} = P_{Cn}, \quad \text{for } n=1.$$

Substituting (3.3) in (3.4) gives,

$$P_{Q_n} = (1 - P_{0n} - P_{1n}) \prod_{i=1}^{n-1} (P_{0i} + P_{1i}), \quad n > 1 \quad (3.5)$$

From the definitions of U and I_j , the total number of decoded packets is obtained as,

$$U = \sum_{j=1}^N I_j \quad (3.6)$$

Taking the expected value of both sides of the above equation, gives the system throughput, $E[U]$, as,

$$E[U] = \sum_{j=1}^N E[I_j] \quad (3.7)$$

From the definition of I_j ,

$$E[I_j] = Prob(I_j = 1) \quad (3.8)$$

$$Prob(I_j = 1) = P_{1j} \prod_{i=1}^{j-1} (P_{0i} + P_{1i})$$

Substituting from eq. (3.2),

$$Prob(I_j = 1) = \lambda p_j e^{-\lambda p_j} \prod_{i=1}^{j-1} (e^{-\lambda p_i} + \lambda p_i e^{-\lambda p_i}), \quad (3.9)$$

$$j > 1.$$

$$Prob(I_1 = 1) = \lambda p_1 e^{-\lambda p_1}$$

Therefore,

$$E[U] = \lambda p_1 e^{-\lambda p_1} + \sum_{j=2}^N \lambda p_j e^{-\lambda p_j} \prod_{i=1}^{j-1} (e^{-\lambda p_i} + \lambda p_i e^{-\lambda p_i}) \quad (3.10)$$

To determine maximum throughput of the system we take partial derivatives of the $E[U]$ in the above with respect to p_i and set the resulting derivatives to zero. We determine p_i 's by solving $(N - 1)$ of those equations simultaneously with the normalization condition $\sum_{i=1}^N p_i = 1$ and $p_i \geq 0, i = 1..N$. We refer to resulting p_i s as optimal access probabilities and they determine the maximum throughput.

2.3.2 Determining received power levels for decoding

In this subsection, we determine the required receive power levels at the BS for successful decoding of the signals. First, we determine the SINR at each power level. Let ϕ_i denote SINR at power level i . Assuming that higher powered signals have been removed from the received signal and that there is a single transmission at power level i , then,

$$\phi_i = \frac{L_i}{N_0 + \sum_{j=i+1}^N \lambda p_j L_j}, \quad i = 1..N \quad (3.11)$$

The summation in the above will be zero if its lower limit is higher than its upper limit. Assuming that the SINR threshold to decode a signal successfully is γ , then we should have,

$$\phi_i \geq \gamma, \quad i = 1..N \quad (3.12)$$

We determine the minimum received power at each level by setting $\phi_i = \gamma$, $i = 1..N$. Then (3.11) gives us N linear equations with N unknowns in $L_i, i = 1..N$. The simultaneous solution of these equations gives us minimum required receive power at each level.

2.3.3 Numerical results

Next, we present numerical results for this case. Initially, we assume that there are two power levels, $N=2$. Fig. 2.1 shows the plot of throughput from (3.10) as a function of the probability that a user chooses power level 1 for transmission with packet arrival rate as a parameter. As may be seen, the throughput of the system drops with increasing probability of users choosing power level 1 as the packet arrival rate increases. It is also seen that maximum throughput depends on the arrival rate and maximum throughput does not occur at equal access probabilities.

Next, we determine the optimal access probabilities and the maximum throughput as explained following eq. (3.10). Fig. 2.2 presents plot of the optimal access probabilities as a function of the packet arrival rate. As may be seen, a user chooses the two power levels with equal probability under light load but the probability that power level 1 is chosen decreases as the traffic load increases. This is essentially a rational choice since if a transmission at power level one is not successful, the transmission at power level two cannot be successful.

Fig. 2.3 presents plot of the throughput as a function of packet arrival rate both for the optimal and uniform access probabilities. In uniform access, a user is equally likely to choose each of the power levels. As may be seen, maximum throughput has a peak at about 2 packets/slot arrival rate for both cases. This peak is slightly higher for optimal than uniform access, although, this peak is slightly lower than twice the maximum throughput of a slotted Aloha channel. While the throughput of the uniform access probability drops to zero as the traffic load increases, the throughput of the optimal access probabilities drops down to the maximum throughput of a slotted Aloha channel. These numerical results validate that the optimal choice of the access probabilities results in better throughput performance and the throughput does not collapse under medium to heavy traffic loads.

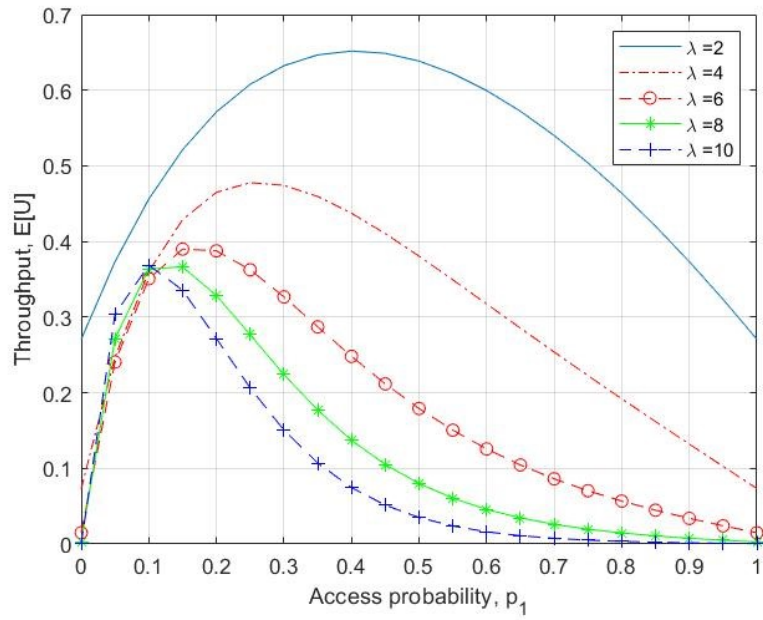


Fig. 2.1. Throughput as a function of probability that a user chooses power level L_1 for $N=2$ power levels with arrival rate as a parameter.

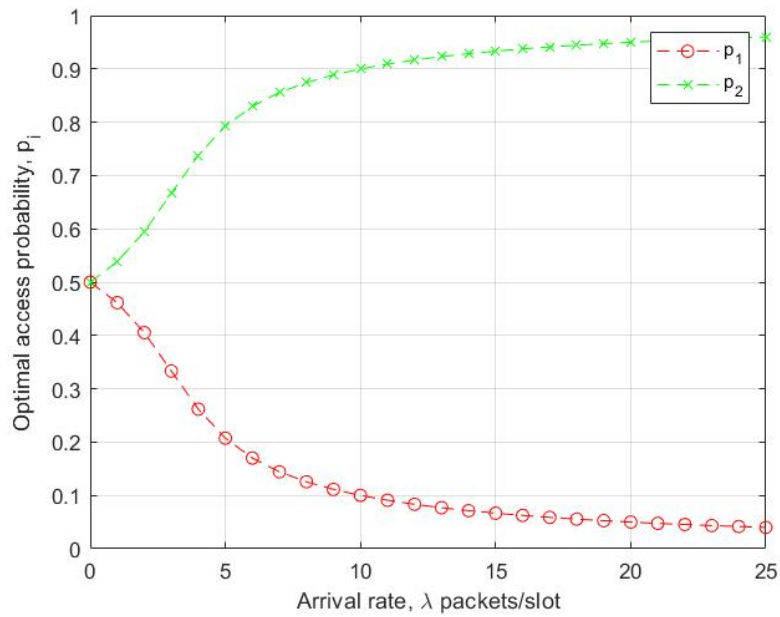


Fig. 2.2. Optimal access probabilities to a power level, p_i , as a function of the traffic arrival rate for $N = 2$ power levels.

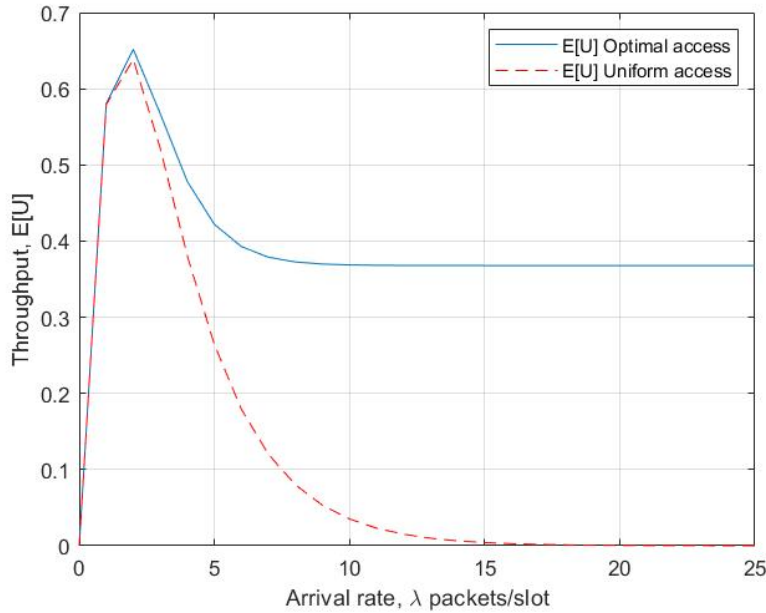


Fig. 2.3. Throughput as a function of packet arrival rate for optimal and uniform access probabilities for $N = 2$ power levels.

Next, we present the corresponding results for $N=3$ power levels. Fig. 2.4 plots the optimal access probabilities as a function of packet arrival rate. The access probabilities have equal values under very light loading, but p_1, p_2 decrease while p_3 increases as the packet arrival rate increases. The optimization keeps reducing values of p_1, p_2 as the arrival rate increases so that successful packet transmission can be maintained at power levels L_1, L_2 .

Fig. 2.5 plots the maximum throughput as a function of packet arrival rate both for optimal and uniform access probabilities. The behavior of the throughput in this figure and the throughput of higher levels are very similar to that in Fig. 2.3. As may be seen, the maximum throughput has a peak that has a value close to three times the maximum of a slotted Aloha channel and it occurs at a arrival rate slightly higher than 2 packets/slot. Also, maximum throughput asymptotically approaches to a value slightly lower than twice the maximum throughput of a slotted ALOHA channel as traffic load increases under optimal access. On the other hand, maximum throughput drops to zero with packet arrival rate under uniform access.

Similar system response is observed for $N = 4, 5$ power levels, wherein the optimization tends to reduce the load in lower power levels and redirect the traffic towards the ultimate power level, which is depicted in Fig 2.6 and Fig. 2.8.

From the above, for any number of power levels N , the throughput is maximized when the system tries to reduce the number of collisions in the preliminary power levels, so that transmission through higher power levels will be successful. It can be seen that maximum throughput has a value slightly less than N times maximum throughput of slotted Aloha protocol. As the packet arrival rate increases maximum throughput decreases but it is lower bounded by $N-1$ times throughput of slotted Aloha protocol.

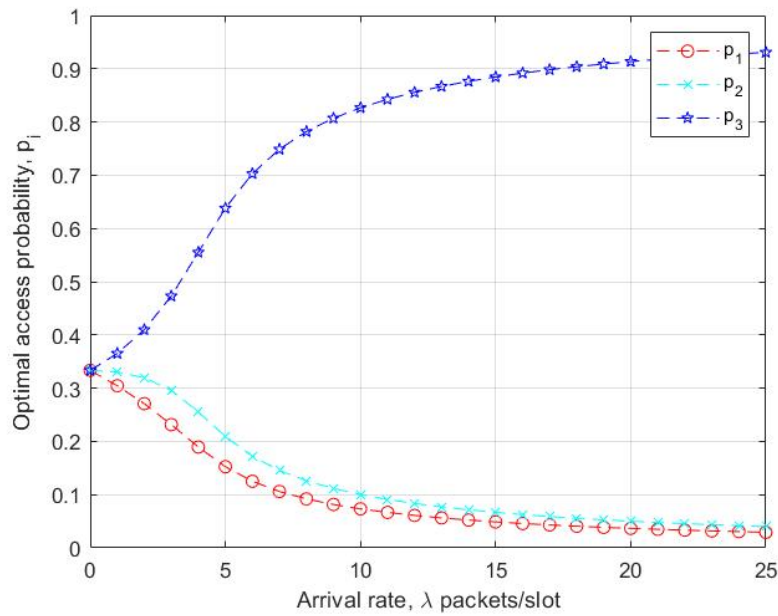


Fig. 2.4. Optimal access probabilities to a power level, p_i , as a function of the traffic arrival rate for $N = 3$ power levels.

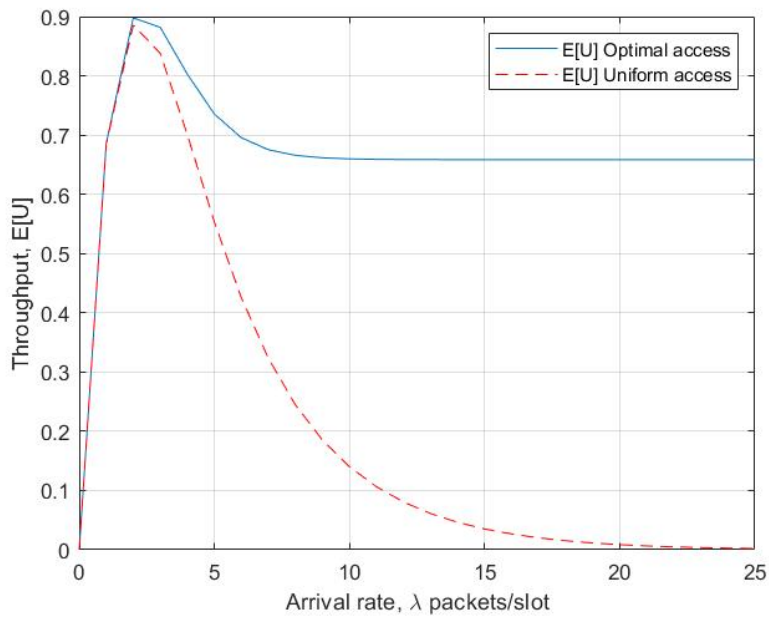


Fig. 2.5. Throughput as a function of packet arrival rate for optimal and uniform access probabilities for $N = 3$ power levels.

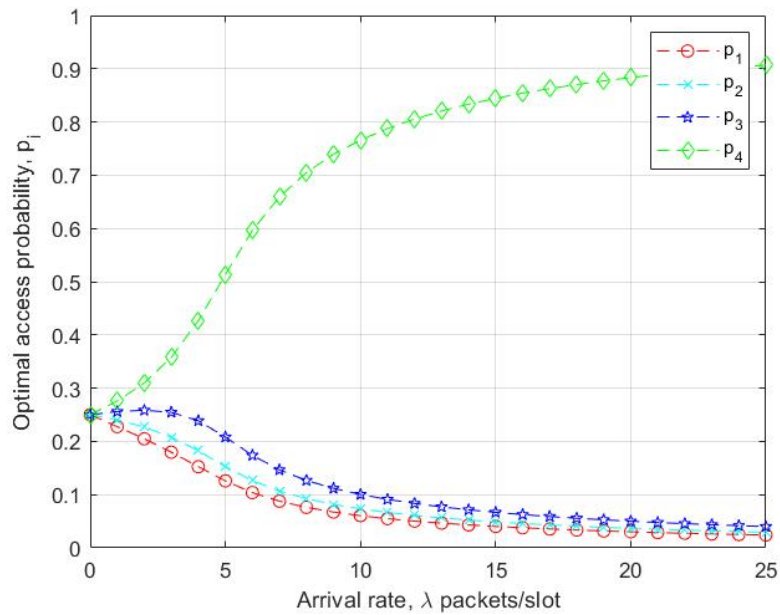


Fig. 2.6. Optimal access probabilities to a power level, p_i , as a function of the traffic arrival rate for $N = 4$ power levels.

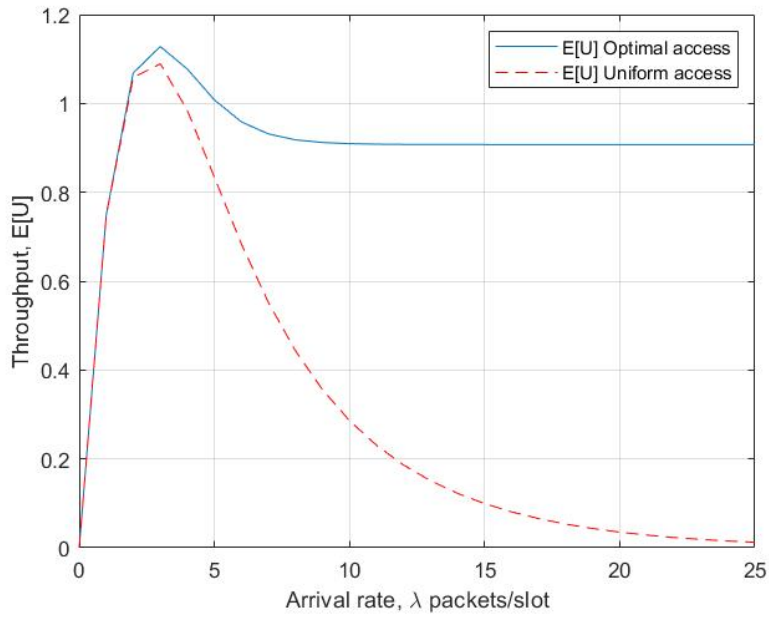


Fig. 2.7. Throughput as a function of packet arrival rate for optimal and uniform access probabilities for $N = 4$ power levels.

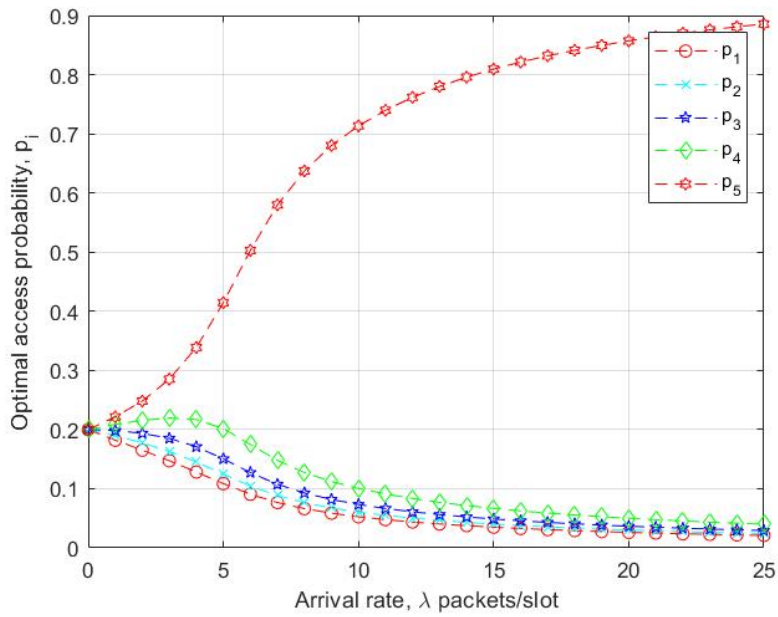


Fig. 2.8. Optimal access probabilities to a power level, p_i , as a function of the traffic arrival rate for $N = 5$ power levels.

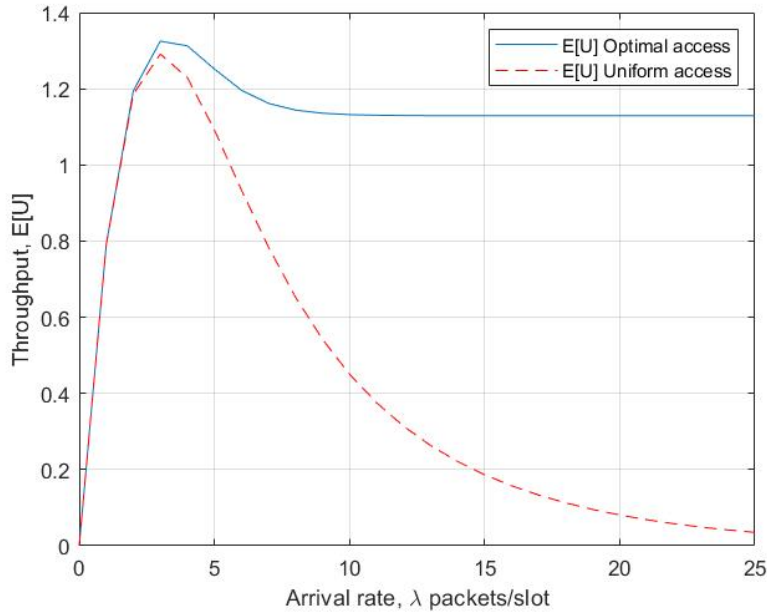


Fig. 2.9. Throughput as a function of packet arrival rate for optimal and uniform access probabilities for $N = 5$ power levels.

2.4 Case 2: A user may not always transmit its packet

The case where a user always transmits in a slot, has the disadvantage that there will be always collision at the N^{th} power level under heavy loads. This could be avoided if a user is given the option of not transmitting during a slot. A packet chosen not to be transmitted will be unsuccessful and will be lost. Clearly, this approach does not benefit the user making this choice, but it improves overall system performance.

2.4.1 Throughput Optimization

The throughput of this scheme is still given by eq. (2.10). Let us define p_0 to denote the probability that a user will choose not to transmit its packet during a slot, then the normalization condition is given by,

$$\sum_{i=0}^N p_i = 1 \quad (3.13)$$

In this case, the optimal access probabilities that maximize the throughput may be determined through the following constrained optimization problem,

$$\begin{aligned} & \max E[U], \\ & \forall \sum_{i=1}^N p_i \leq 1, p_i \geq 0, i = 1..N \end{aligned} \quad (3.14)$$

The p_0 is determined from eq. (3.13) after the solution of the above optimization problem. We note that the equations (3.11), (3.12) still apply in determining the minimum power levels for this case.

2.4.2 Numerical results

From the solution of optimization problem in eq. (3.14), we obtain the optimal access probabilities and the maximum throughput for systems with $N=2, 4$ and 6 power levels. Fig. 2.10 to Fig. 2.12 plot optimal access probabilities as a function of the packet arrival rate for each of the power levels. As may be seen, probability that a user will choose not to transmit its packet, p_0 , is zero under light loading but increases as the load increases. Fig. 2.13 presents the throughput of the system as a function of the packet arrival rate for $N=2, 3, 4$ and 6 , respectively. It may be seen that the throughput of the system initially increases with the traffic load until it reaches to a plateau. From the comparison of the curves for $N=2$ in Fig. 2.3 and Fig. 2.7, this plateau occurs at the peak of the previous case where each user always transmits during a slot.

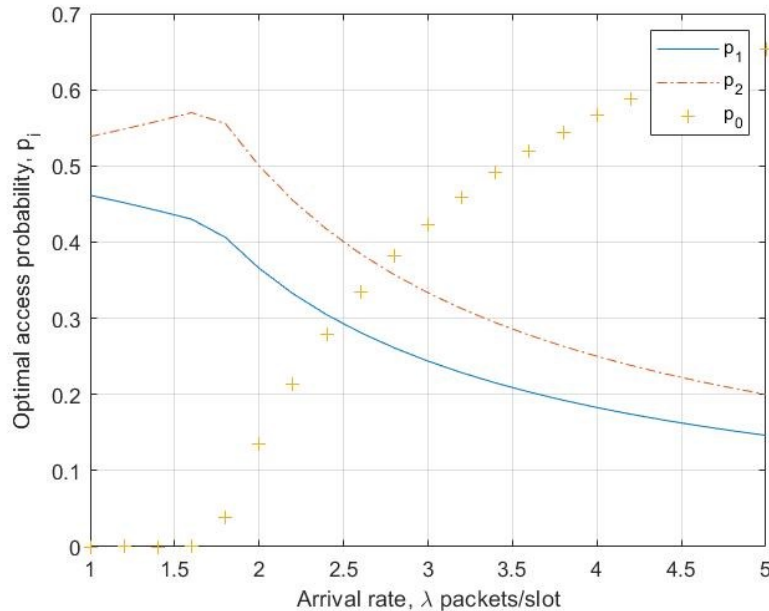


Fig. 2.10. Optimal access probabilities as a function of the packet arrival rate for $N = 2$ power levels.

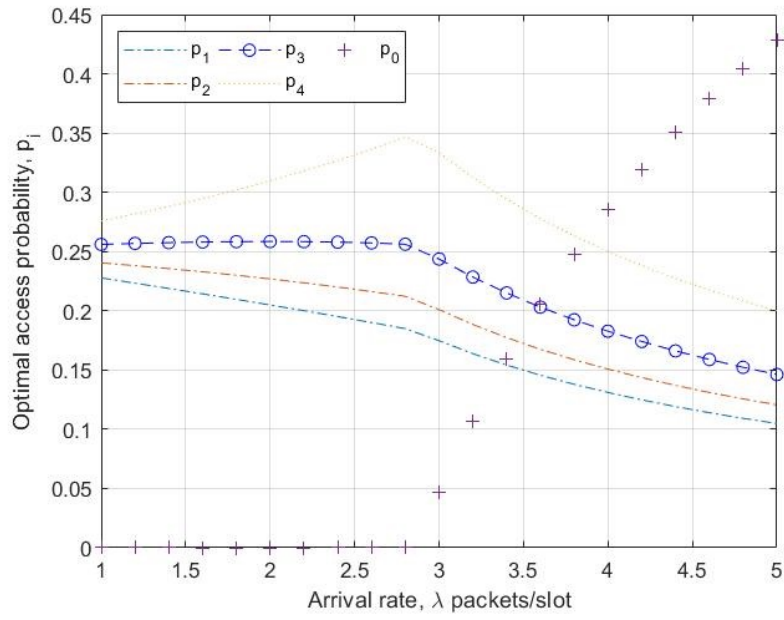


Fig. 2.11. Optimal access probabilities as a function of packet arrival rate for $N = 4$ power levels.

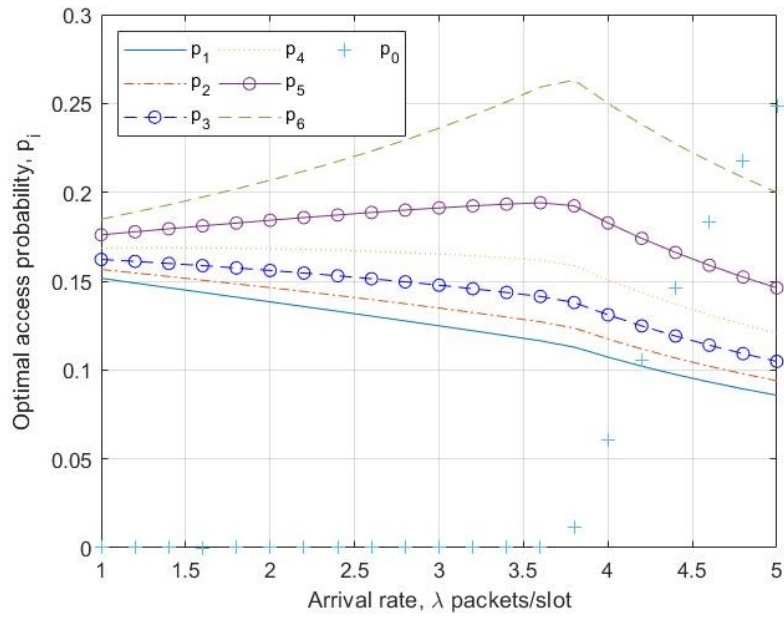


Fig. 2.12. Optimal access probabilities as a function of packet arrival rate for $N = 6$ power levels.

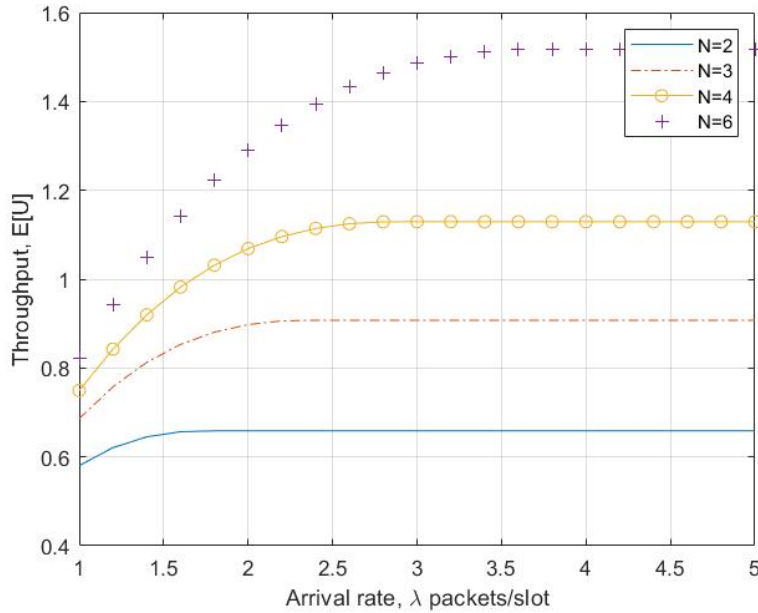


Fig. 2.13. Throughput as a function of the packet arrival rate for $N=2, 3, 4$ and 6 power levels

2.4.3 Determining received power for Level 1 decoding

Next, we present results for the received power for level one, L_1 , assuming that a user may choose not to transmit its packet. We assumed that the noise spectral density is normalized to $N_0 = 1$. We note that in these figures received signal at lowest power level equals to the SINR threshold value, $L_N = \gamma$, and the value corresponds to the required received power if the user was the only one accessing to the channel. Fig. 2.14 plots L_1 as a function of packet arrival rate for different SINR threshold values, and $N=4$. It may be seen that the required power level increases initially with the packet arrival rate but then it levels off. It is also seen that $L_1 \gg L_N$ as the arrival rate increases. Fig. 2.15 plots L_1 as a function of the number of power levels, N , for a fixed value of SINR threshold and packet arrival rate as a parameter. It is again seen that L_1 increases with the number of power levels. Fig. 2.16 presents averaged received power as a function of the packet arrival rate for $N=4$ power levels and SINR as a parameter. NOMA provides better performance but at the expense of higher power consumption.

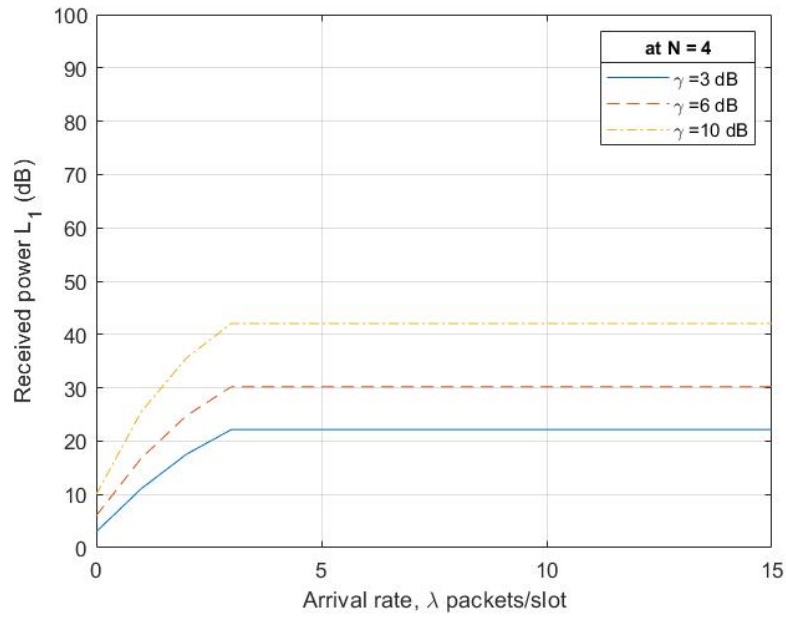


Fig. 2.14. Received power level L_1 as a function of the packet arrival rate for $N=4$ power levels with threshold SINR as a parameter.

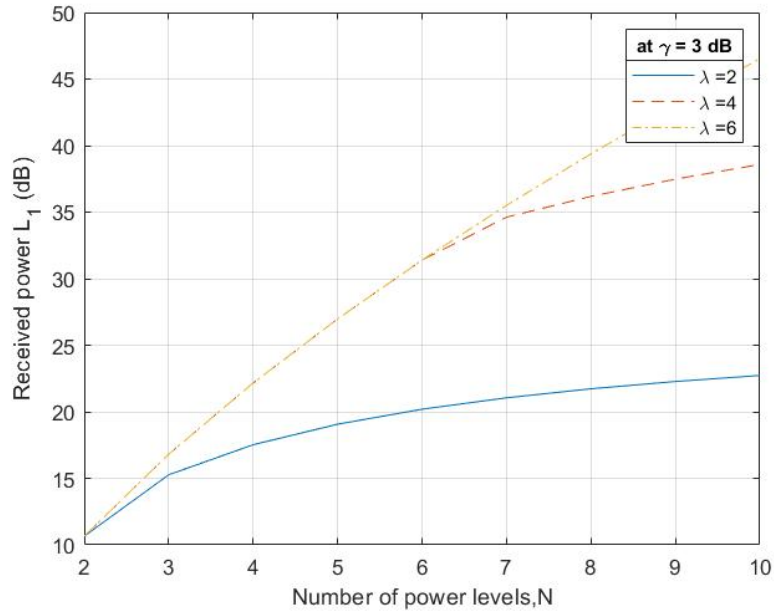


Fig. 2.15. Received power at power level L_1 as a function of the number of power levels for fixed value of SINR, $\gamma = 3$ and packet arrival rate as a parameter.

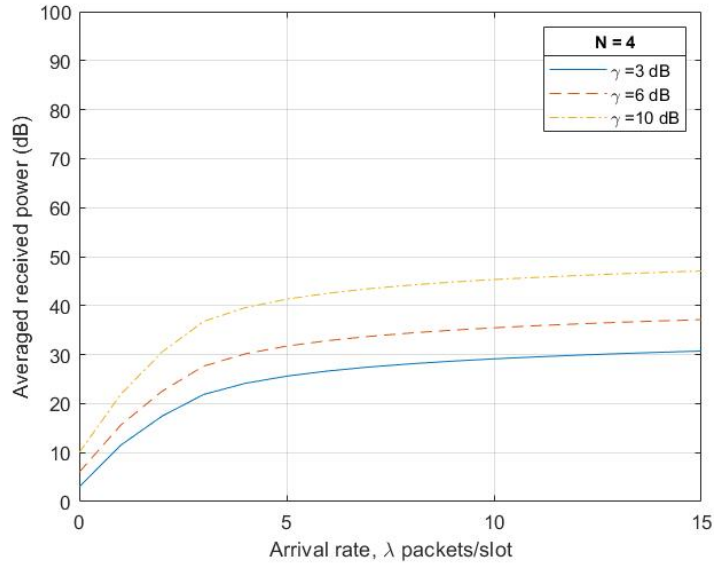


Fig. 2.16. Average received power level L_1 as a function of the packet arrival rate for $N=4$ power levels with threshold SINR as a parameter.

2.5 Conclusion

In this chapter, we studied a single channel slotted Aloha PD-NOMA system with packet loss. The new packets arrive to the system according to a Poisson process and each packet belongs to a different user. Each packet is transmitted only once and if the transmission is not successful, then the packet is lost. We devised an optimization problem that maximizes the overall throughput of the system with the user access probabilities to the power levels as variables. The solution of the optimization problem results in the optimal access probabilities that maximizes the throughput. It is shown that this optimization provides better throughput performance compared to uniform access to the power levels. The maximum throughput is almost N times higher than maximum throughput of slotted Aloha protocol for a system with N power levels and it decreases with increasing arrival rate but it is lower bounded by $N-1$ times maximum throughput of slotted Aloha protocol. The optimization is also altered for optional transmission of packets which reduces the loss of packets and thus, increases the throughput and efficiency of the system. In this case, the maximum throughput has the same value as non-optional packet transmission case, but maximum throughput does not drop with increasing arrival rate. We have also determined the minimum required received power at the BS for the highest power level. It is shown that the required received power increases with the number of power levels and with the traffic load.

Chapter 3

Modeling of a NOMA system without packet losses

3.1 Introduction

This chapter extends the results of the previous chapter to a NOMA system without packet losses. As before each user may only have a single packet to transmit at any time. The users choose a power level randomly and transmit their packets synchronously. A packet remains in the system until successfully decoded by the receiver. The optimal power level choice that maximizes throughput of the system is determined and compared with uniform choice of power levels under two cases. In one case, a user always has to transmit its packet and in the other case it may choose not to transmit its packet. The required received power levels for decoding at the receiver are also determined.

However, in this model, we assume that the packets that cannot be transmitted successfully during a slot remains in the system. Thus, in each slot, the left-over packets from the previous slot and new arriving packets contend for transmission. As before it is assumed that each packet belongs to a different user. The objective of the following analysis is determining the PGF of the distribution of the number of packets in the system assuming that the access probabilities are chosen optimally in each slot such that the number of packets transmitted during that slot is maximized. As a result, the optimal access probabilities during a slot will depend on the number of packets contending during that slot.

3.2 Mathematical model

The model of the previous chapter presented in section 2.1 remains valid in this chapter. In summary, there are N power levels and L_i denotes the received power at level i at the base station. The time-axis is slotted, and the transmission time of a packet takes a single slot. It is assumed that each user may have a single packet to transmit during a slot, therefore the number of

users with packets and total number of packets to be transmitted during a slot are same. The received signal at level i has higher power than the signal at level $i+1$, $L_i > L_{i+1}$ and a user chooses to transmit its packet at power level L_i with probability p_i during a slot. It is assumed that the arrival of new users with packets to transmit during a slot is given by a Poisson distribution with parameter λ packets/slot. The transmission of a packet will be successful if the packet can be decoded by the receiver. A packet will remain in the system until it can be decoded successfully by the receiver. In each slot, leftover packets from the previous slot and new arriving packets will contend for successful transmission. Next let us introduce the new notation needed for the analysis,

n_i : number of packets in the system at the end of i^{th} slot.

a_i : number of new arriving packets to the system during slot i .

I_i : number of packets successfully transmitted during slot i .

M

: maximum number of contending packets for which success probability is not constant.

$A_m = \text{Prob}(m \text{ new users with packets arriving during a slot}).$

$q_{kj} = \text{Prob}(j \text{ successful packet transmissions during a slot given that there were } k \text{ packets at the beginning of a slot})$

$q_j = \text{Prob}(j \text{ packets being transmitted successfully during a slot})$

$\pi_k = \text{Prob}(\text{there are } k \text{ packets in the system at the steady-state}).$

We note that q_{kj} will be zero for $k < j$. Since at most a single packet may be transmitted at each power level, then $j \leq N$. Let us define matrix of transition probabilities of q_{kj} referred as success probabilities, for upto k packets in the system,

$$Q_k = \begin{bmatrix} q_{00} & \cdots & q_{0N} \\ \vdots & \ddots & \vdots \\ q_{k0} & \cdots & q_{kN} \end{bmatrix} \quad (3.1)$$

3.2.1 Derivation of the PGF of the number of packets in the system

In this section, we will derive PGF of the number of packets in the system at the steady-state. We choose the end of slots as the imbedding points, then the number of packets in the system at the end of $i+1^{\text{st}}$ slot is given by the following equation,

$$n_{i+1} = n_i - I_{i+1} + a_{i+1} \quad (3.2)$$

where $I_{i+1} \leq \min(n_i, N)$.

Let us define, $Q_i(z)$ as the PGF of the distribution of the number of packets in the system at the end of i^{th} slot, then,

$$Q_i(z) = E[z^{n_i}] = \sum_{k=0}^{\infty} z^k \text{Prob}(n_i = k) \quad (3.3)$$

Then from eq. (3.2),

$$Q_{i+1}(z) = E[z^{n_i - I_{i+1} + a_{i+1}}] \quad (3.4)$$

We assume that the number of new arrivals during a slot are independent of the number of packets in the system, further number of arrivals in each slot are independent of the arrivals in the other slots,

$$Q_{i+1}(z) = E[z^{n_i - I_{i+1}}]A(z) \quad (3.5)$$

where, $A(z) = E[z^{a_i}]$

$$E[z^{n_i - I_{i+1}}] = \sum_{k=0}^{\infty} \sum_{j=0}^N z^{k-j} \text{Prob}(n_i = k, I_{i+1} = j) \quad (3.6)$$

$$E[z^{n_i - I_{i+1}}] = \sum_{k=0}^{\infty} \sum_{j=0}^N z^{k-j} \text{Prob}(I_{i+1} = j | n_i = k) \text{Prob}(n_i = k)$$

We know that,

$$q_{kj} = \text{Prob}(I_{i+1} = j | n_i = k)$$

$$E[z^{n_i - I_{i+1}}] = \sum_{k=0}^{\infty} \sum_{j=0}^N z^{k-j} q_{kj} \text{Prob}(n_i = k) \quad (3.7)$$

We expect that as k gets larger, probabilities q_{kj} asymptotically will become independent of k . Let us assume that for some value of M , probabilities q_{kj} become independent of k . Since

maximum number of packets that can be successfully transmitted is N , clearly, we should have $M > N$.

Let us assume that $q_{kj} = q_{(M+1)j}$ for $k > M$ and let $q_j = q_{(M+1)j}$, as a result, the above equation may be written as,

$$E[z^{n_i - I_{i+1}}] = \sum_{k=0}^M \sum_{j=0}^N z^{k-j} q_{kj} \text{Prob}(n_i = k) + \sum_{k=M+1}^{\infty} \sum_{j=0}^N z^{k-j} q_{kj} \text{Prob}(n_i = k) \quad (3.8)$$

$$E[z^{n_i - I_{i+1}}] = \sum_{k=0}^M \sum_{j=0}^N z^{k-j} q_{kj} \text{Prob}(n_i = k) + \sum_{k=M+1}^{\infty} \sum_{j=0}^N z^{k-j} q_j \text{Prob}(n_i = k) \quad (3.9)$$

$$E[z^{n_i - I_{i+1}}] = \sum_{k=0}^M \sum_{j=0}^N z^{k-j} q_{kj} \text{Prob}(n_i = k) + \sum_{j=0}^N z^{-j} q_j \sum_{k=M+1}^{\infty} z^k \text{Prob}(n_i = k)$$

$$E[z^{n_i - I_{i+1}}] = \sum_{k=0}^M \sum_{j=0}^N z^{k-j} q_{kj} \text{Prob}(n_i = k) + \sum_{j=0}^N z^{-j} q_j [Q_i(z) - \sum_{k=0}^M z^k \text{Prob}(n_i = k)] \quad (3.10)$$

Substituting eq. (3.10) in eq. (3.5) gives,

$$Q_{i+1}(z) = \left\{ \sum_{k=0}^M \sum_{j=0}^N z^{k-j} q_{kj} \text{Prob}(n_i = k) + \sum_{j=0}^N z^{-j} q_j [Q_i(z) - \sum_{k=0}^M z^k \text{Prob}(n_i = k)] \right\} A(z) \quad (3.11)$$

At the steady-state,

Let $\pi_k = \text{Prob}(n = k)$

$$Q(z) = E[z^n] = \sum_{k=0}^{\infty} z^k \text{Prob}(n = k) \quad (3.12)$$

Taking limit in eq. (3.11) as $i \rightarrow \infty$,

$$Q(z) = \frac{\left\{ z^N \left\{ \sum_{k=0}^M \sum_{j=0}^N z^{k-j} q_{kj} \pi_k \right\} - \left\{ \sum_{j=0}^N z^{N-j} q_j \sum_{k=0}^M z^k \pi_k \right\} \right\} A(z)}{z^N - \sum_{j=0}^N q_j z^{N-j} A(z)} \quad (3.13)$$

The above equation gives us PGF of the number of packets in the system at the steady-state. However, the above PGF has $(M+1)$ unknowns, π_k , $k = 0..M$. The denominator of the PGF has N roots within the unit circle. One of those roots is zero, which is also a root of the numerator. However, the other roots give us $N-1$ equations. Thus, we need $M+1-(N-1) = M+2-N$ more equations to determine the unknowns.

Next, we will apply the normalization condition $Q(z)|_{z=1} = 1$ to determine one of the equations involving the unknowns. Since $Q(z)|_{z=1}$ results in $0/0$ indeterminacy, we apply L'Hôpital's rule,

$$\left\{ \left\{ \sum_{k=0}^M \sum_{j=0}^N q_{kj} \pi_k \left((k-j+N) z^{(k-j+N-1)} \right) - \sum_{j=0}^N q_j z^{N-j} \sum_{k=0}^M k z^{k-1} \pi_k - \sum_{j=0}^N q_j (N-j) z^{N-j-1} \sum_{k=0}^M z^k \pi_k \right\} A(z) + \left\{ z^N \left\{ \sum_{k=0}^M \sum_{j=0}^N z^{k-j} q_{kj} \pi_k \right\} - \left\{ \sum_{j=0}^N z^{N-j} q_j \sum_{k=0}^M z^k \pi_k \right\} \right\} A'(z) = N z^{N-1} - \left[A(z) \sum_{j=0}^N (N-j) z^{N-j-1} q_j + A'(z) \sum_{j=0}^N z^{N-j} q_j \right] \right\} \Big|_{z=1} \quad (3.14)$$

After substituting $z = 1$ in the above,

$$\sum_{k=0}^M \sum_{j=0}^N q_{kj} \pi_k (k-j+N) - \sum_{j=0}^N q_j \sum_{k=0}^M k \pi_k - \sum_{j=0}^N q_j (N-j) \sum_{k=0}^M \pi_k = N - \left[\sum_{j=0}^N (N-j) q_j + A'(1) \sum_{j=0}^N q_j \right] \quad (3.15)$$

Since $\sum_{j=0}^N q_j = 1$, we have the following equation derived from the normalization condition,

$$\sum_{k=0}^M \sum_{j=0}^N q_{kj} \pi_k (k-j+N) - \sum_{k=0}^M k \pi_k - \sum_{j=0}^N (N-j) q_j \sum_{k=0}^M \pi_k = N - \sum_{j=0}^N (N-j) q_j - A'(1) \quad (3.16)$$

3.2.2 Application of homogeneous Markov chain analysis

Since the number of packets in the system follows a Markov chain at the end of slots, the steady-state distribution of the number of packets also satisfies the following equation,

$$\pi = \pi P \quad (3.17)$$

where, $\pi = [\pi_0, \dots, \pi_k \dots]$ and P is the transition probability matrix of the system. From eq. (3.17),

$$\pi_k = \sum_{i=0}^k \sum_{j=0}^i \pi_i q_{ij} A_{k-(i-j)} + \sum_{i=k+1}^{k+N} \pi_k q_{i(i-k)} A_0, \quad k = 0..M+1-N \quad (3.18)$$

We note that the above $M+2-N$ equations only involve the unknowns π_k , $k = 0..M$ and thus do not introduce any new unknowns. Thus, these equations together with the equations from the roots of the denominator provide enough number of equations to determine all the unknowns.

3.2.3 Average mean packet delay

Next, we will determine average number of users in the system, \bar{n} , which is given by,

$$\bar{n} = \left. \frac{dQ(z)}{dz} \right|_{z=1}$$

Let us write $Q(z)$ in eq. (3.13) as,

$$Q(z) = \frac{U}{V},$$

Where,

$$U = \left\{ z^N \left\{ \sum_{k=0}^M \sum_{j=0}^N z^{k-j} q_{kj} \pi_k \right\} - \left\{ \sum_{j=0}^N z^{N-j} q_j \sum_{k=0}^M z^k \pi_k \right\} \right\} A(z)$$

$$V = z^N - \sum_{j=0}^N q_j z^{N-j} A(z)$$

Thus,

$$\frac{dQ(z)}{dz} = \frac{VU' - UV'}{V^2} \quad (3.19)$$

The above equation leads to $0/0$ indeterminate form at $z=1$ because $V|_{z=1} = 0$ and $U|_{z=1} = 0$.

Thus, we apply L'Hôpital's rule,

$$\frac{dQ(z)}{dz} = \frac{VU'' - UV''}{2VV'} \quad (3.20)$$

The above also results in the indeterminate form at $z=1$, as a result applying L'Hôpital's rule again to eq. (3.20),

$$\frac{dQ(z)}{dz} = \frac{VU''' + V'U'' - UV''' - U'V''}{2[VV'' + (V')^2]}$$

Thus, average number of users in the system is given by,

$$\bar{n} = \left. \frac{dQ(z)}{dz} \right|_{z=1} = \left. \frac{V'U'' - U'V''}{2(V')^2} \right|_{z=1} \quad (3.21)$$

Where,

$$U' = \left\{ \begin{array}{l} A'(z) \left\{ \sum_{k=0}^M \sum_{j=0}^N z^{k-j+N} q_{kj} \pi_k \right\} - \left\{ \sum_{j=0}^N q_j \sum_{k=0}^M z^{k-j+N} \pi_k \right\} \\ + A(z) \left\{ \begin{array}{l} \sum_{k=0}^M \sum_{j=0}^N q_{kj} \pi_k \left((k-j+N) z^{(k-j+N-1)} \right) \\ - \sum_{j=0}^N \sum_{k=0}^M q_j \pi_k \left((k-j+N) z^{(k-j+N-1)} \right) \end{array} \right\} \end{array} \right\}$$

$$V' = Nz^{N-1} - [A(z) \sum_{j=0}^N (N-j) z^{N-j-1} q_j + A'(z) \sum_{j=0}^N z^{N-j} q_j]$$

$$U'|_{z=1} = A'(1) \sum_{k=0}^M \sum_{j=0}^N q_{kj} \pi_k - \sum_{k=0}^M \pi_k \sum_{j=0}^N \sum_{k=0}^M q_j \pi_k (k-j+N) - \sum_{j=0}^N \sum_{k=0}^M q_j \pi_k (k-j+N)$$

$$V'|_{z=1} = N - \sum_{j=0}^N (N-j) q_j - A'(1)$$

$$\begin{aligned} U''|_{z=1} = A'(1) & \left\{ \sum_{k=0}^M \sum_{j=0}^N (q_{kj} - q_j) \pi_k ((k-j+N)) \right\} \\ & + A'(1) \left\{ \sum_{k=0}^M \sum_{j=0}^N (q_{kj} - q_j) \pi_k ((k-j+N)) \right\} \\ & + \left\{ \sum_{k=0}^M \sum_{j=0}^N (q_{kj} - q_j) \pi_k ((k-j+N)(k-j+N-1)) \right\} \end{aligned}$$

$$V''|_{z=1} = \sum_{k=0}^M \sum_{j=0}^N q_{kj} \pi_k (k-j+N) - \sum_{j=0}^N \sum_{k=0}^M q_j \pi_k (k-j+N) \quad (3.22)$$

Finally, from the Little's formula mean packet delay is given by,

$$\bar{d} = \frac{\bar{n}}{\lambda} \quad (3.23)$$

Next, we will consider three methods for user access to the power levels. We will determine user access probabilities to power levels for each of these methods.

3.2.4 User access probabilities

First, we will determine the throughput of the system, average number of packets that may be successfully transmitted during a slot, for a given number of packets in the system. Then, we will consider three methods for the user choice of power levels. Next, we will determine q_{kj} as a function of the access probabilities for each value of k . Let us define,

k_i : number of packets choosing power level i .

$\vec{k} = (k_1, \dots, k_i, \dots, k_N)$ = the components of this vector correspond to the number of users choosing each power level.

The joint distribution of the number of users that has chosen each power level is given by the multinomial distribution,

$$f(\vec{k}) = \binom{k}{\vec{k}} \prod_{i=1}^N p_i^{k_i}$$

where , $k = \sum_{i=1}^N k_i$.

Let i^* denote the power level that the first collision occurs, it means no collision in power levels, $i = 1..i^* - 1$. This means that $k_i \leq 1$ for $i = 1..i^* - 1$.

$u_{\vec{k}}$ = number of packets successfully transmitted at the system state \vec{k} . Then,

$$u_{\vec{k}} = \sum_{i=1}^{i^*-1} k_i \tag{3.24}$$

and,

$$Prob(u_{\vec{k}}) = f(\vec{k}) \tag{3.25}$$

Let us define U_k as the number of successfully transmitted packets given that there are k contending packets. Then, we have,

$$q_{kj} = Prob(U_k = j) \tag{3.26}$$

but we have,

$$Prob(U_k = j) = \sum_{\forall (u_{\vec{k}}=j)} \vec{k} Prob(u_{\vec{k}} = j)$$

Substituting from eq. (3.25)

$$Prob(U_k = j) = \sum_{\forall (u_{\vec{k}}=j)} \vec{k} f(\vec{k}) \tag{3.27}$$

but we have,

$$q_{kj} = Prob(U_k = j)$$

Then expected number of packets successfully transmitted is given by,

$$E[U_k] = \sum_{j=0}^N j q_{kj} \quad (3.28)$$

$$E[U_k] = \sum_{j=0}^N j \sum_{\substack{\vec{k} \\ \forall (u_{\vec{k}}=j)}} f(\vec{k}) \quad (3.29)$$

Thus, the above equation determines throughput of the system, average number of packets that may be transmitted during a slot, for given number of packets in the system as a function of the user access probabilities for the choice of power levels. Next, we will consider three methods for the choice of user access probabilities.

3.3 Methods of determining user access probabilities

3.3.1 Optimal User access probabilities with non-optional transmit

3.3.1.1 Analysis

In this method, a user chooses access probabilities such that throughput of the system is maximized for a given number of packets in the system. In this method, all the users with packets transmit their packets in each slot. Thus, we determine values of user access probabilities that maximizes average number of packets that may be successfully transmitted during a slot. We take partial derivatives of $E[U_k]$ wrt access probabilities and set them to zero. Simultaneous solution of $(N-1)$ of those equations together with the normalization condition determine optimal access probabilities.

$$\frac{\partial E[U_k]}{\partial p_i} = 0 \quad , \quad i = 1..N \quad \text{and} \quad \sum_{i=1}^N p_i = 1$$

Then, we determine optimal transmit probabilities from eq. (3.26) using these access probabilities for given number of packets.

3.3.1.2 Numerical results and Discussion

First, we give results for the case of $N=2$ power levels. We determine the optimal access probabilities through solution of the maximization problem in eq. (3.28). Fig. 3.1 plots optimal access probabilities as a function of the number of packets in the system. As may be seen the users

are equally likely to choose either power level for the number of packets $k \leq 2$ in the system and, from there on, they choose power level two with increasing probability with the number of packets in the system. Then, we determine the transition probabilities q_{kj} from eq. (3.26) and eq. (3.27) for the optimal access probabilities. Fig. 3.2 plots these optimal transition probabilities as a function of the number of packets in the system. As anticipated, these transition probabilities become independent of the number of packets in the system for $M > 6$. The corresponding truncated transition probability matrix, Q , is given in eq. (3.30). The transition probabilities q_{kj} will be given by, $q_j = q_{7j}$, for $j = 0, 1, 2$ for all values of $k \geq M$. Fig. 3.3 plots the maximum throughput per slot as a function of the number of packets in the system. It may be seen that maximum throughput levels off for $M > 6$.

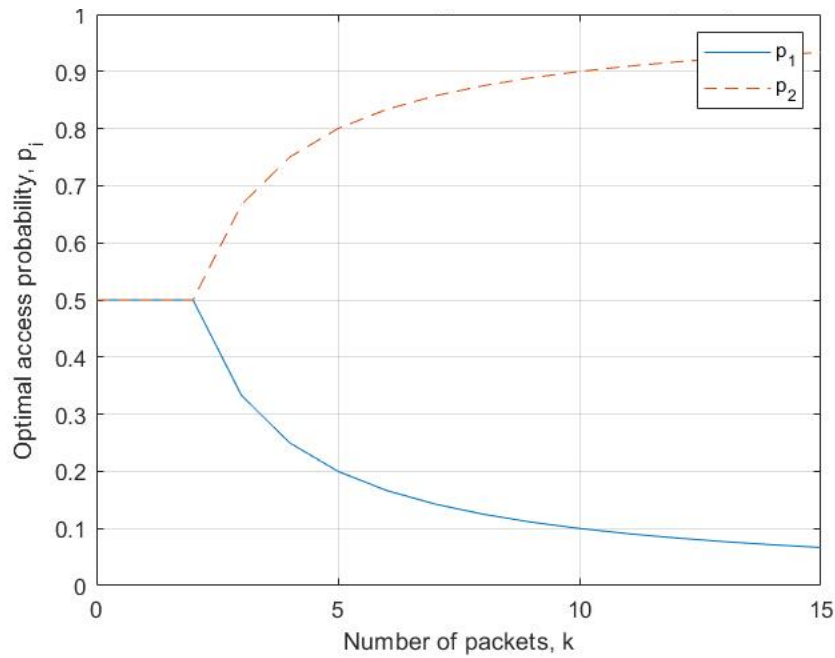


Fig. 3.1. Optimal access probabilities as a function of the number of packets in the system for $N=2$ power levels

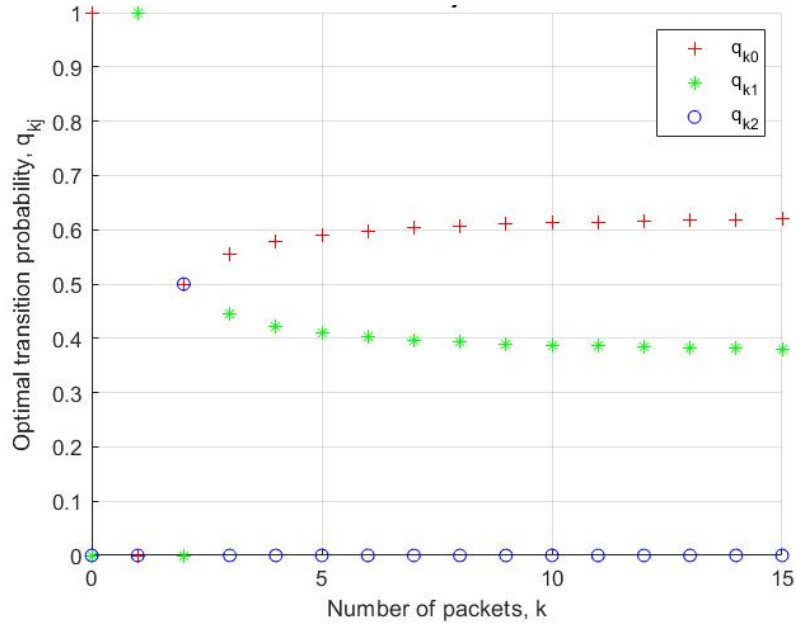


Fig. 3.2. Success probabilities as a function of number of packets for \$N=2\$ power levels

$$Q_{M+1} = \begin{bmatrix} q_{00} & q_{01} & q_{02} \\ q_{10} & q_{11} & q_{12} \\ q_{20} & q_{21} & q_{22} \\ q_{30} & q_{31} & q_{32} \\ q_{40} & q_{41} & q_{42} \\ q_{50} & q_{51} & q_{52} \\ q_{60} & q_{61} & q_{62} \end{bmatrix} \Rightarrow Q_{M+1} = \begin{bmatrix} 1 & 0 & 0 \\ 0 & 1 & 0 \\ 0.5 & 0 & 0.5 \\ 0.5556 & 0.4444 & 0 \\ 0.5781 & 0.4219 & 0 \\ 0.5904 & 0.4096 & 0 \\ 0.5981 & 0.4019 & 0 \end{bmatrix} \quad (3.30)$$

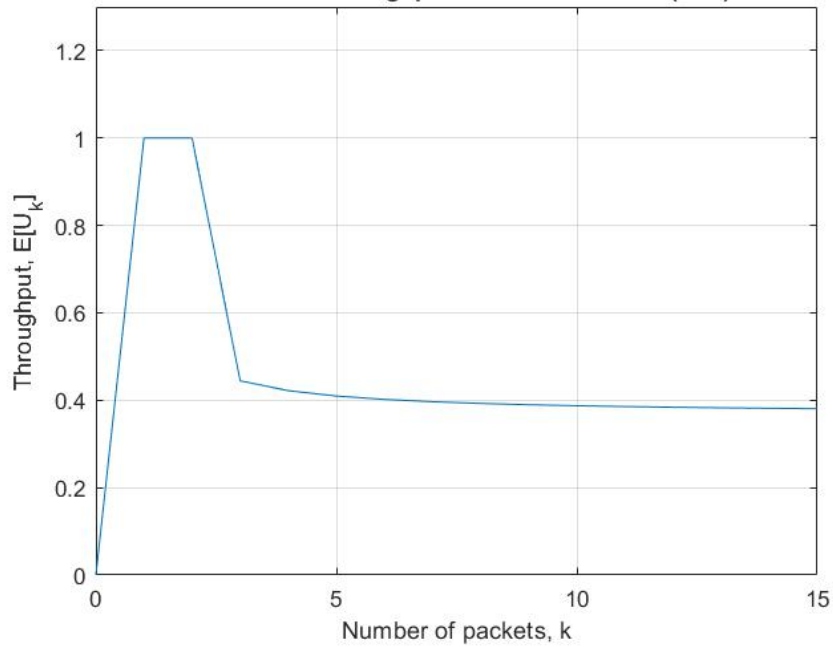


Fig. 3.3. Throughput as a function of the packet arrival rate for \$N=2\$ power levels

The response of the system with power levels $N > 2$, is akin to that of what has been discussed above. Fig. 3.4 depicts the optimal access probabilities of the system when $N = 3$. It can be seen that the users have almost equal probability of choosing a power level p_i , at lighter loads, whereas, the optimization lets the system choose higher power level with a higher probability in order to retain maximum throughput. The optimal transition probabilities, q_{kj} , in this case, has a striking increase for $j \leq 2$, and eventually becoming independent of the number of packets in the system, k , when $M > 7$. This result is outlined in fig. 3.5. The resulting truncated Q matrix is given by eq. (3.31).

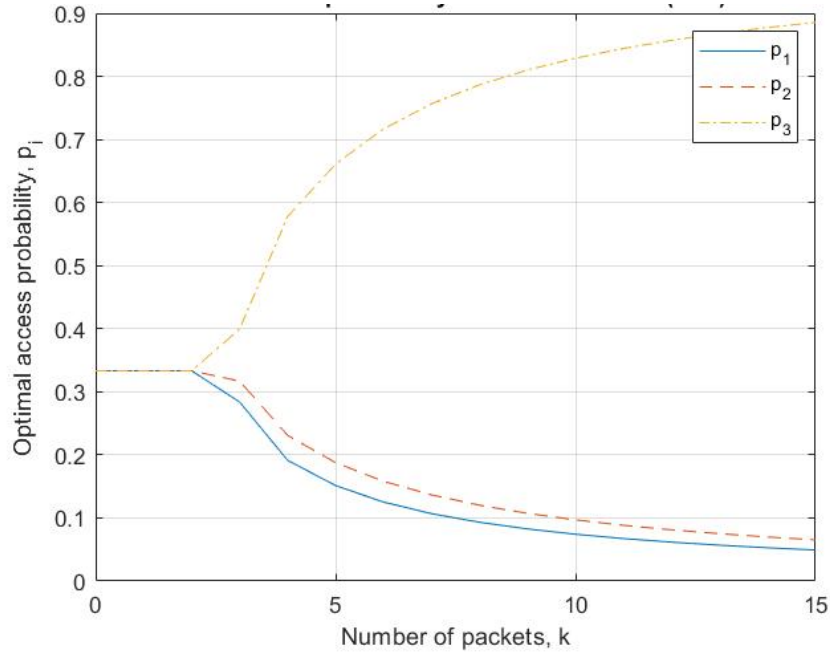


Fig. 3.4. Optimal access probabilities as a function of the number of packets in the system for $N=3$ power levels

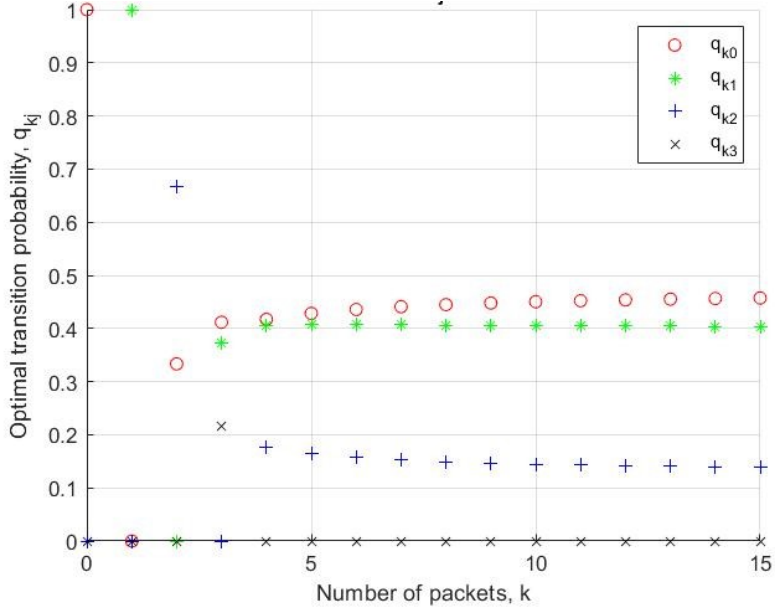


Fig. 3.5. Success probabilities as a function of number of packets for N=3 power levels

$$Q_{M+1} = \begin{bmatrix} q_{00} & q_{01} & q_{02} & q_{03} \\ q_{10} & q_{11} & q_{12} & q_{13} \\ q_{20} & q_{21} & q_{22} & q_{23} \\ q_{30} & q_{31} & q_{32} & q_{33} \\ q_{40} & q_{41} & q_{42} & q_{43} \\ q_{50} & q_{51} & q_{52} & q_{53} \\ q_{60} & q_{61} & q_{62} & q_{63} \\ q_{70} & q_{71} & q_{72} & q_{73} \end{bmatrix} \Rightarrow Q_{M+1} = \begin{bmatrix} 1 & 0 & 0 & 0 \\ 0 & 1 & 0 & 0 \\ 0.3333 & 0 & 0.6667 & 0 \\ 0.4116 & 0.3729 & 0 & 0.2155 \\ 0.4171 & 0.4058 & 0.1770 & 0 \\ 0.4283 & 0.4076 & 0.1640 & 0 \\ 0.4357 & 0.4075 & 0.1566 & 0 \\ 0.4410 & 0.4070 & 0.1519 & 0 \end{bmatrix} \quad (3.31)$$

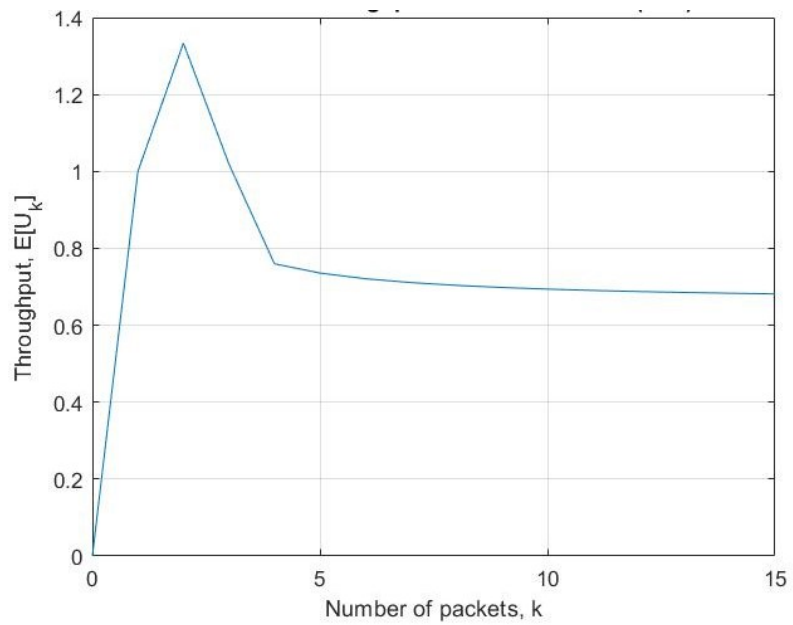


Fig. 3.6. Throughput as a function of the packet arrival rate for N=3 power levels

Next, we present corresponding results for a system with $N = 4$ and $N = 5$ power levels. Fig. 3.7 and fig. 3.10 plots optimal access probabilities as a function of the number of packets in the system. Fig. 3.8 and fig. 3.11 plots these optimal transition probabilities as a function of the number of packets in the system. It may be seen that these transition probabilities become independent of the number of packets in the system for $M > 9$ and $M > 12$, respectively. The corresponding truncated transition probability matrix, Q , is given in eq. (3.32) and eq. (3.33). Fig. 3.9 and fig. 3.12 plots the maximum throughput as a function of the number of packets in the system.

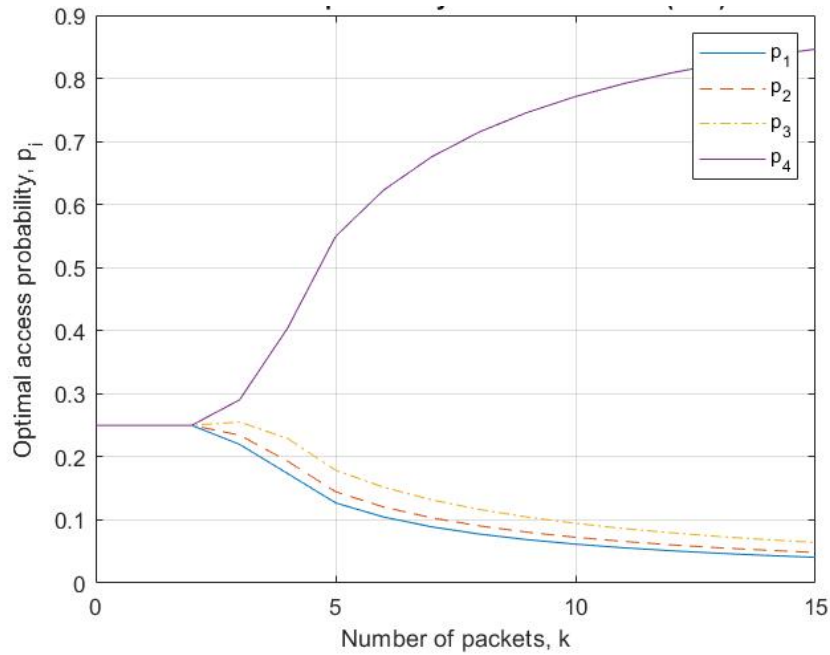


Fig. 3.7. Optimal access probabilities as a function of the number of packets in the system for $N=4$ power levels

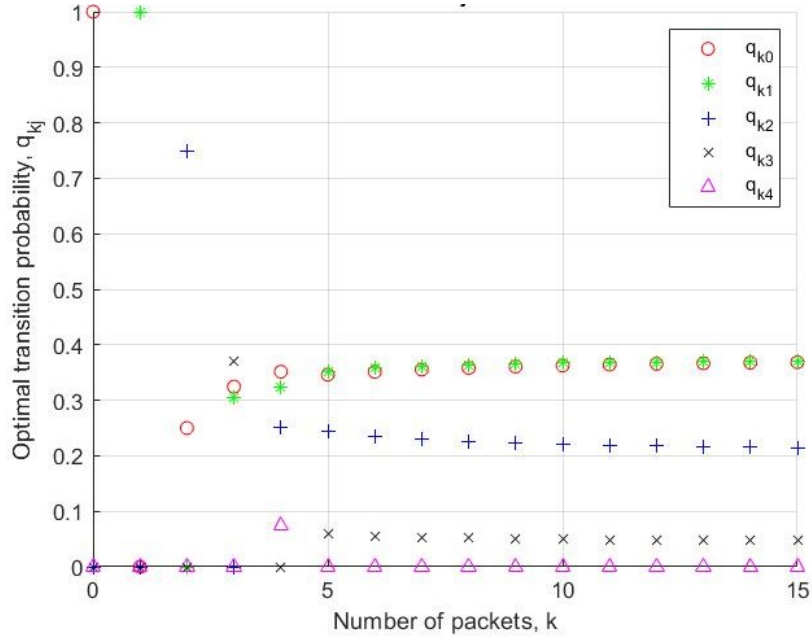


Fig. 3.8. Success probabilities as a function of number of packets for $N=4$ power levels

$$Q_{M+1} = \begin{bmatrix} q_{00} & q_{01} & q_{02} & q_{03} & q_{04} \\ q_{10} & q_{11} & q_{12} & q_{13} & q_{14} \\ q_{20} & q_{21} & q_{22} & q_{23} & q_{24} \\ q_{30} & q_{31} & q_{32} & q_{33} & q_{34} \\ q_{40} & q_{41} & q_{42} & q_{43} & q_{44} \\ q_{50} & q_{51} & q_{52} & q_{53} & q_{54} \\ q_{60} & q_{61} & q_{62} & q_{63} & q_{64} \\ q_{70} & q_{71} & q_{72} & q_{73} & q_{74} \\ q_{80} & q_{81} & q_{82} & q_{83} & q_{84} \\ q_{90} & q_{91} & q_{92} & q_{93} & q_{94} \end{bmatrix} \Rightarrow \begin{bmatrix} 1 & 0 & 0 & 0 & 0 \\ 0 & 1 & 0 & 0 & 0 \\ 0.2500 & 0 & 0.7500 & 0 & 0 \\ 0.3245 & 0.3046 & 0 & 0.3708 & 0 \\ 0.3514 & 0.3225 & 0.2515 & 0 & 0.0745 \\ 0.3461 & 0.3506 & 0.2436 & 0.0595 & 0 \\ 0.3513 & 0.3577 & 0.2353 & 0.0555 & 0 \\ 0.3552 & 0.3617 & 0.2297 & 0.0531 & 0 \\ 0.3583 & 0.3643 & 0.2258 & 0.0515 & 0 \\ 0.3607 & 0.3660 & 0.2229 & 0.0503 & 0 \end{bmatrix} \quad (3.32)$$

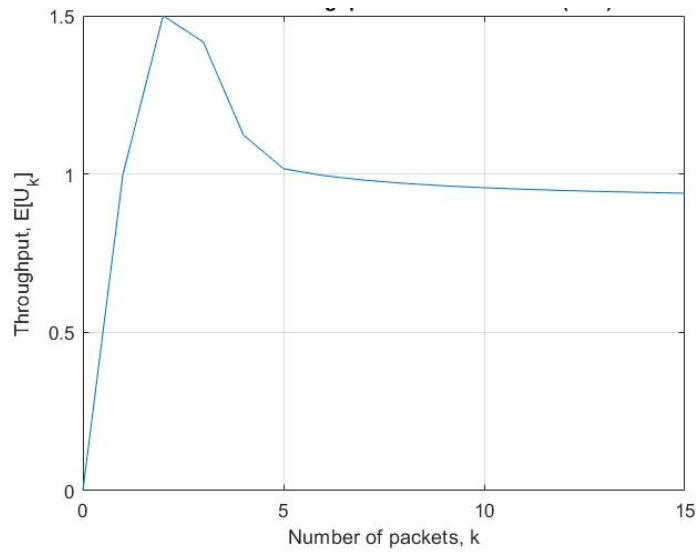


Fig. 3.9. Throughput as a function of the packet arrival rate for $N=4$ power levels

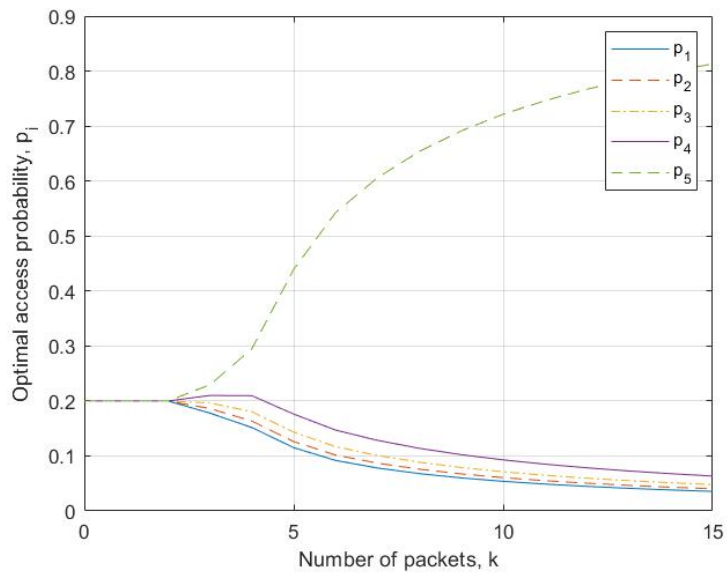


Fig. 3.10. Optimal access probabilities as a function of the number of packets in the system for $N=5$ power levels

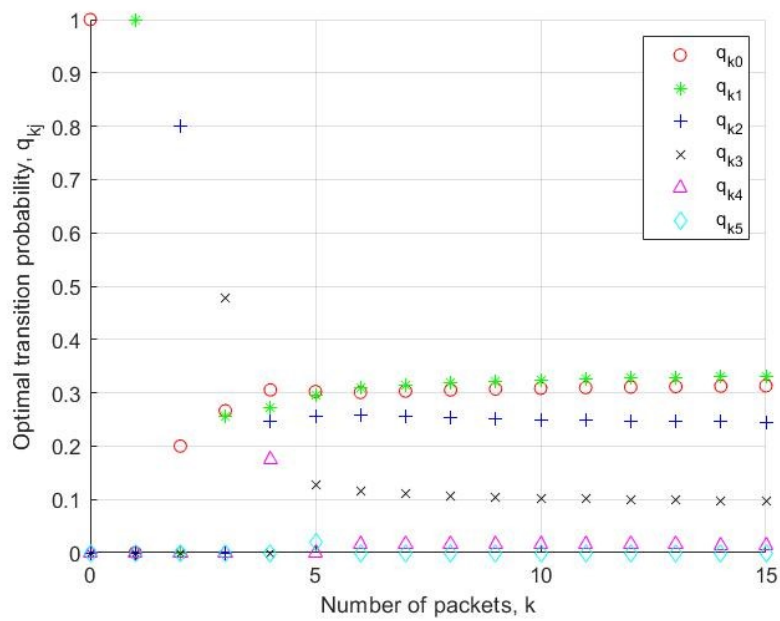


Fig. 3.11. Success probabilities as a function of number of packets for $N=5$ power levels

$$Q_{M+1} = \begin{bmatrix} q_{00} & q_{01} & q_{02} & q_{03} & q_{04} & q_{05} \\ q_{10} & q_{11} & q_{12} & q_{13} & q_{14} & q_{15} \\ q_{20} & q_{21} & q_{22} & q_{23} & q_{24} & q_{25} \\ q_{30} & q_{31} & q_{32} & q_{33} & q_{34} & q_{35} \\ q_{40} & q_{41} & q_{42} & q_{43} & q_{44} & q_{45} \\ q_{50} & q_{51} & q_{52} & q_{53} & q_{54} & q_{55} \\ q_{60} & q_{61} & q_{62} & q_{63} & q_{64} & q_{65} \\ q_{70} & q_{71} & q_{72} & q_{73} & q_{74} & q_{75} \\ q_{80} & q_{81} & q_{82} & q_{83} & q_{84} & q_{85} \\ q_{90} & q_{91} & q_{92} & q_{93} & q_{94} & q_{95} \\ q_{10,0} & q_{10,1} & q_{10,2} & q_{10,3} & q_{10,4} & q_{10,5} \\ q_{11,0} & q_{11,1} & q_{11,2} & q_{11,3} & q_{11,4} & q_{11,5} \\ q_{12,0} & q_{12,1} & q_{12,2} & q_{12,3} & q_{12,4} & q_{12,5} \end{bmatrix} \Rightarrow \begin{bmatrix} 1 & 0 & 0 & 0 & 0 & 0 \\ 0 & 1 & 0 & 0 & 0 & 0 \\ 0.2 & 0 & 0.8 & 0 & 0 & 0 \\ 0.2664 & 0.2565 & 0 & 0.4770 & 0 & 0 \\ 0.3054 & 0.2730 & 0.2462 & 0 & 0.1752 & 0 \\ 0.3024 & 0.2946 & 0.2555 & 0.1280 & 0 & 0.0193 \\ 0.3006 & 0.3087 & 0.2575 & 0.1160 & 0.0170 & 0 \\ 0.3031 & 0.3151 & 0.2549 & 0.1103 & 0.0163 & 0 \\ 0.3052 & 0.3193 & 0.2527 & 0.1066 & 0.0159 & 0 \\ 0.3070 & 0.3224 & 0.2509 & 0.1040 & 0.0155 & 0 \\ 0.3084 & 0.3246 & 0.2494 & 0.1020 & 0.0153 & 0 \\ 0.3097 & 0.3264 & 0.2482 & 0.1005 & 0.0151 & 0 \\ 0.3107 & 0.3277 & 0.2472 & 0.0992 & 0.0149 & 0 \end{bmatrix} \quad (3.33)$$

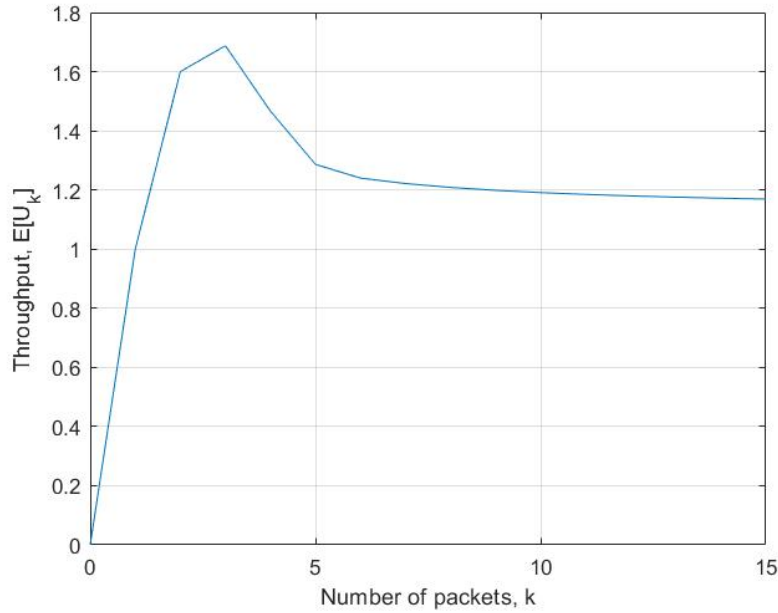


Fig. 3.12. Throughput as a function of the packet arrival rate for $N=5$ power levels

3.3.2 Optimal user access probabilities with optional transmit

3.3.2.1 Analysis

In Section 3.3.1, a user with a packet will always transmit its packet during a slot. That method has the disadvantage that at high loads there will be always collisions at the N^{th} power level. This could be avoided if a user is given the option of not transmitting during a slot. Evidently, there is no benefit to the user that chooses not to transmit its packet during a slot, but this will improve overall system performance.

The analysis section 3.3.1 will slightly be modified to apply to this method. We handle this method by introducing an imaginary power level for users choosing not to transmit. Let us change the notation as follows,

- p_i : probability of user accessing power level i , $i = 0, \dots, N$.
- k_i : the number of users choosing power level i , $i = 0, \dots, N$.
- $\vec{k} = (k_0, \dots, k_i, \dots, k_N)$ = vector of the number of users choosing each power level.

Thus, power level L_0 is the imaginary power level for those users that choose not to transmit during a slot. The joint distribution of the number of users that has chosen each power level is given by the multinomial distribution,

$$f(\vec{k}) = \binom{k}{\vec{k}} \prod_{i=0}^N p_i^{k_i}$$

As before i^* denotes the power level that the first collision occurs at power levels $i = 1..N$ which excludes power level zero. The remainder of equations (eq. (3.24) – eq. (3.29)) remain same and optimal user access probabilities are determined by maximizing average number of packets that may be transmitted during a slot, $E[U_k]$, given that there were k packets. Then, optimal user access probabilities may be determined as in Method i) but including power level zero,

$$\frac{\partial E[U_k]}{\partial p_i} = 0 \quad , \quad i = 0..N \quad \text{and} \quad \sum_{i=0}^N p_i = 1$$

3.3.2.2 Numerical results and Discussion

First, we give results for the case of $N=2$ power levels. Fig. 3.13 plots optimal access probabilities from the solution of the maximization problem as a function of the number of packets in the system. It can be seen that the probability that a user will choose not to transmit, p_0 , soars up significantly as the number of contending packets during a slot increase. This implies that the system is more inclined towards not transmitting a packet when the packet queue grows. Fig. 3.14 plots the optimal transition probabilities as a function of the number of packets in the system. The graph illustrates that even for high number of packets in the system probability that a packet will be successfully transmitted at power level N is nonzero. Also, it is seen that the transition probabilities become independent of the number of packets in the system for $M > 6$. The corresponding truncated transition probability matrix, Q , is given in eq. (3.34). Fig. 3.15 plots the

maximum throughput as a function of the number of packets in the system. It may be seen that maximum throughput levels off for $M > 6$.

Owing to the change in the Q matrix of the system, it is evident from comparing fig. 3.3 and fig. 3.15 that, though the throughput is identical for lighter loads, there is a significant increase in the throughput when the system is optimized for optional transmission of packets.

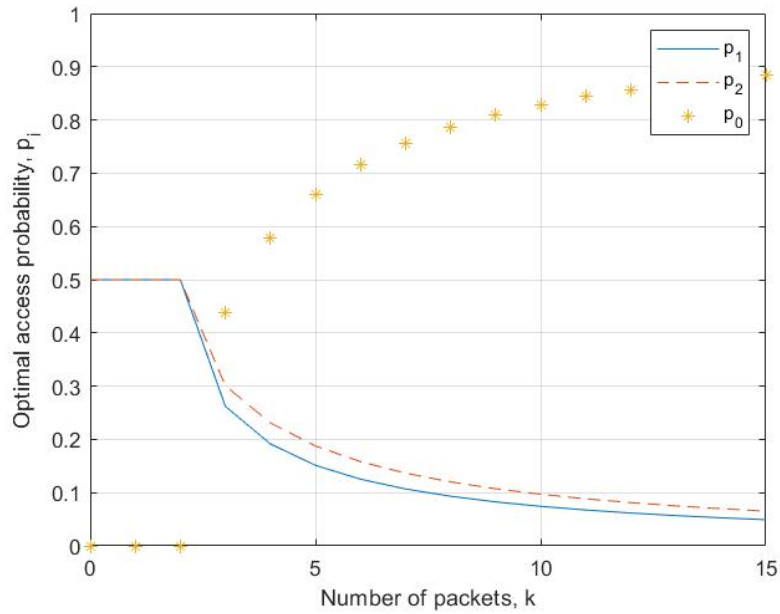


Fig. 3.13. Optimal access probabilities as a function of the number of packets in the system for $N=2$ power levels

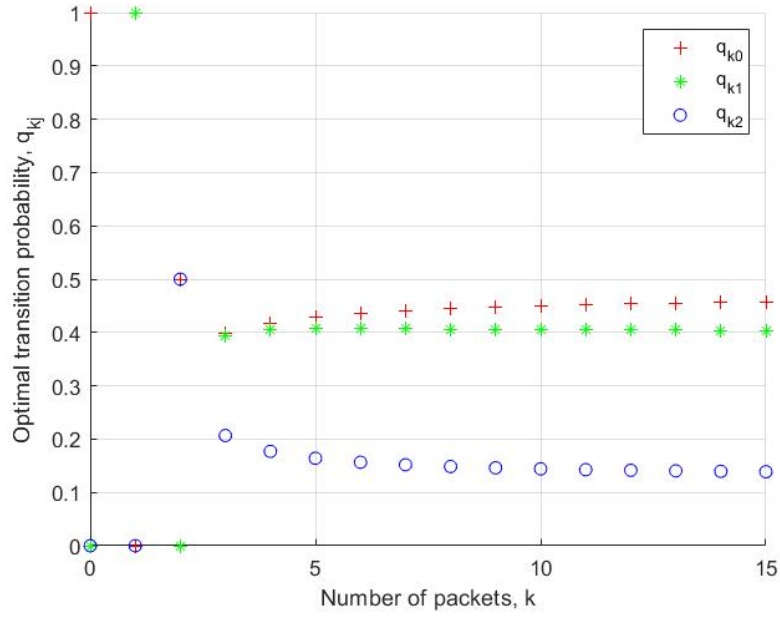


Fig. 3.14. Success probabilities as a function of number of packets for $N=2$ power levels

$$Q_{M+1} = \begin{bmatrix} q_{00} & q_{01} & q_{02} \\ q_{10} & q_{11} & q_{12} \\ q_{20} & q_{21} & q_{22} \\ q_{30} & q_{31} & q_{32} \\ q_{40} & q_{41} & q_{42} \\ q_{50} & q_{51} & q_{52} \\ q_{60} & q_{61} & q_{62} \end{bmatrix} \quad Q_{M+1} = \begin{bmatrix} 1 & 0 & 0 \\ 0.0001 & 0.9999 & 0 \\ 0.5 & 0 & 0.5 \\ 0.3994 & 0.3938 & 0.2067 \\ 0.4171 & 0.4058 & 0.1770 \\ 0.4283 & 0.4076 & 0.1640 \\ 0.4357 & 0.4075 & 0.1566 \end{bmatrix} \quad (3.34)$$

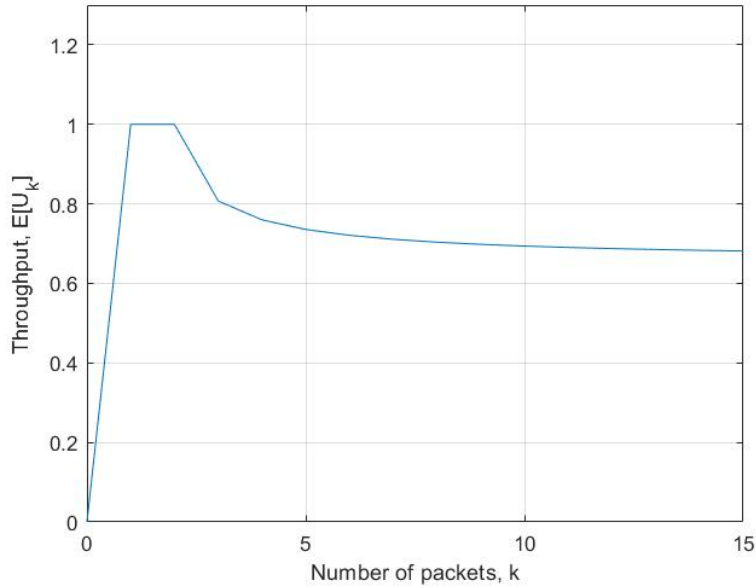


Fig. 3.15. Throughput as a function of the packet arrival rate for $N=2$ power levels

Fig. 3.16 elucidates the variation of optimal access probabilities in the case of optional transmission of packets, when the number of power levels in the system $N = 3$. An increase in the value of p_0 is clearly inferred as the number of packets in the system increase. Fig. 3.17 plots the optimal transition probabilities as a function of number of packets in the system. As clearly illustrated by the curve, we have the Q matrix that is not varied by the increase in the number of packets in the system when $M > 7$. The truncated Q matrix for the same is given by eq. (3.35). Fig. 3.18 shows the throughput of the system as a function of the number of packets in the system. A comparison similar to that of $N = 2$, can be drawn between Fig. 3.6 and Fig. 3.18, which infers an improvement in the system efficiency.

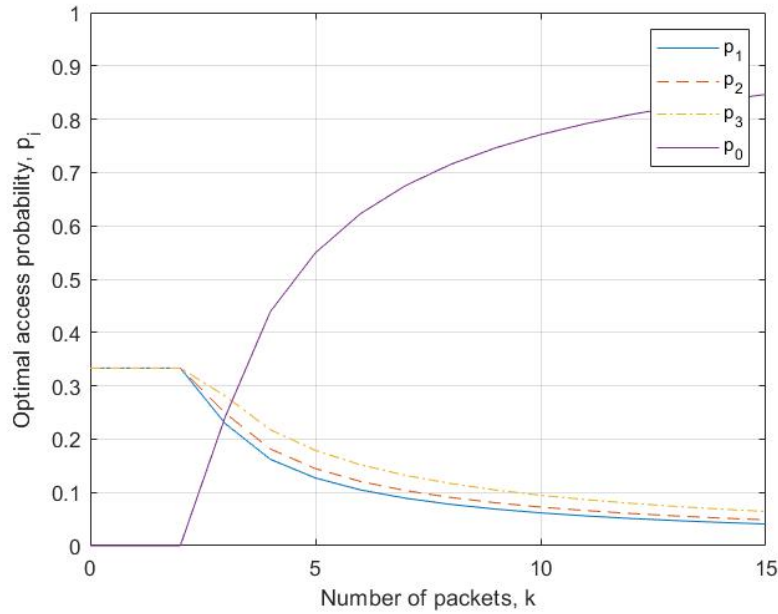


Fig. 3.16. Optimal access probabilities as a function of the number of packets in the system for $N=3$ power levels

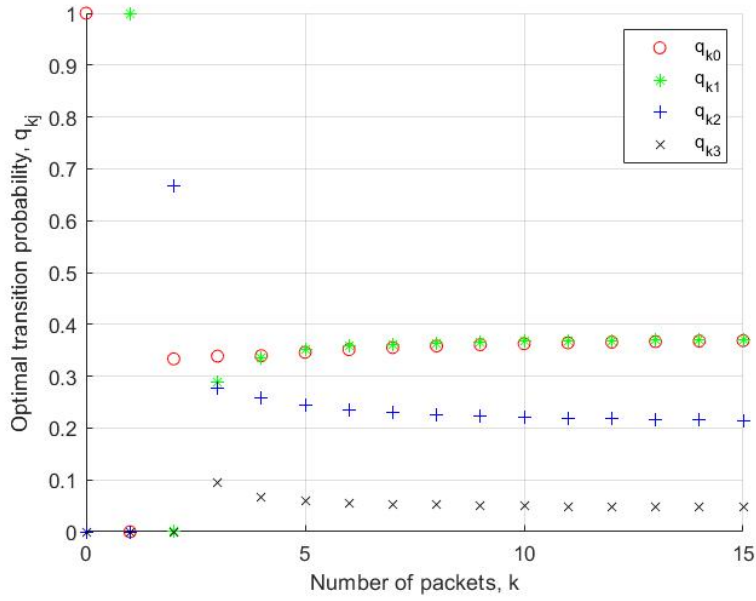


Fig. 3.17. Success probabilities as a function of number of packets for $N=3$ power levels

$$Q_{M+1} = \begin{bmatrix} q_{00} & q_{01} & q_{02} & q_{03} \\ q_{10} & q_{11} & q_{12} & q_{13} \\ q_{20} & q_{21} & q_{22} & q_{23} \\ q_{30} & q_{31} & q_{32} & q_{33} \\ q_{40} & q_{41} & q_{42} & q_{43} \\ q_{50} & q_{51} & q_{52} & q_{53} \\ q_{60} & q_{61} & q_{62} & q_{63} \\ q_{70} & q_{71} & q_{72} & q_{73} \end{bmatrix} \Rightarrow Q_{M+1} = \begin{bmatrix} 1 & 0 & 0 & 0 \\ 0.0001 & 0.9999 & 0 & 0 \\ 0.3333 & 0.0001 & 0.6666 & 0 \\ 0.3386 & 0.2884 & 0.2772 & 0.0956 \\ 0.3396 & 0.3355 & 0.2574 & 0.0673 \\ 0.3461 & 0.3506 & 0.2436 & 0.0595 \\ 0.3513 & 0.3577 & 0.2353 & 0.0555 \\ 0.3552 & 0.3617 & 0.2297 & 0.0531 \end{bmatrix} \quad (3.35)$$

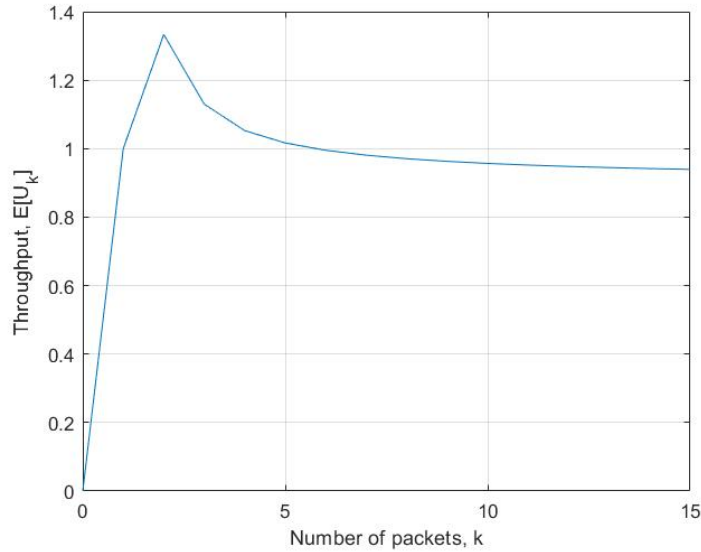


Fig. 3.18. Throughput as a function of the packet arrival rate for $N=3$ power levels

The system behavior is similar as N increases and the results are elucidated for number of power levels $N = 4$, in Fig. 3.19, Fig. 3.20 and Fig. 3.21. One can observe an increase in the overall throughput of the system, as illustrated in Fig. 3.21. Eq. (3.36) gives the truncated Q matrix for the system in this case. The results for $N = 5$ is outlined in Fig. 3.22, Fig. 3.23, and Fig. 3.24

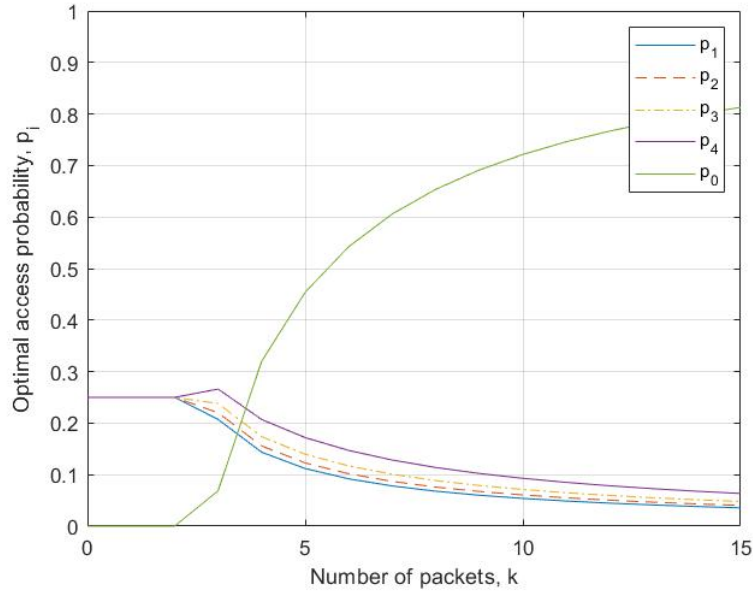


Fig. 3.19. Optimal access probabilities as a function of the number of packets in the system for $N=4$ power levels

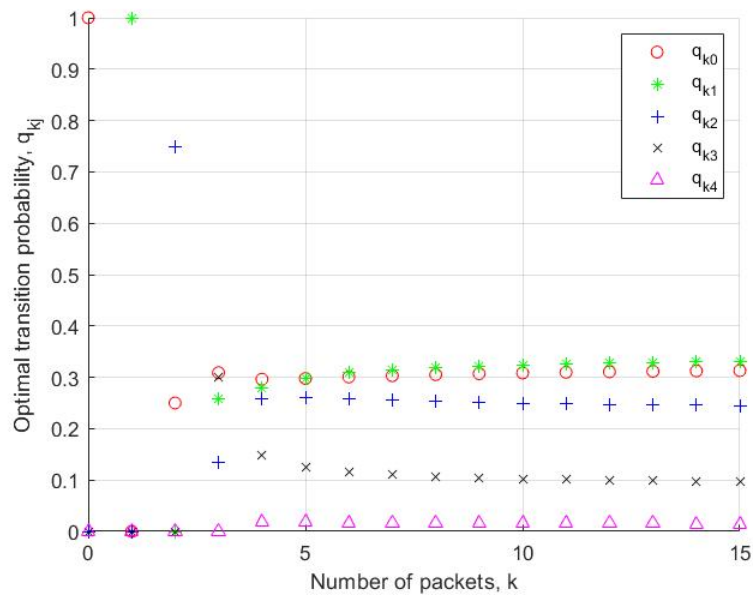


Fig. 3.20. Success probabilities as a function of number of packets for $N=4$ power levels

$$Q_{M+1} = \begin{bmatrix} q_{00} & q_{01} & q_{02} & q_{03} & q_{04} \\ q_{10} & q_{11} & q_{12} & q_{13} & q_{14} \\ q_{20} & q_{21} & q_{22} & q_{23} & q_{24} \\ q_{30} & q_{31} & q_{32} & q_{33} & q_{34} \\ q_{40} & q_{41} & q_{42} & q_{43} & q_{44} \\ q_{50} & q_{51} & q_{52} & q_{53} & q_{54} \\ q_{60} & q_{61} & q_{62} & q_{63} & q_{64} \\ q_{70} & q_{71} & q_{72} & q_{73} & q_{74} \\ q_{80} & q_{81} & q_{82} & q_{83} & q_{84} \\ q_{90} & q_{91} & q_{92} & q_{93} & q_{94} \end{bmatrix} \Rightarrow \begin{bmatrix} 1 & 0 & 0 & 0 & 0 \\ 0.0001 & 0.9999 & 0 & 0 & 0 \\ 0.2499 & 0.0001 & 0.7499 & 0 & 0 \\ 0.3089 & 0.2571 & 0.1335 & 0.3002 & 0 \\ 0.2961 & 0.2785 & 0.2579 & 0.1408 & 0.0193 \\ 0.2978 & 0.2982 & 0.2601 & 0.1258 & 0.0179 \\ 0.3006 & 0.3087 & 0.2575 & 0.1160 & 0.0170 \\ 0.3031 & 0.3151 & 0.2549 & 0.1103 & 0.0163 \\ 0.3052 & 0.3193 & 0.2527 & 0.1066 & 0.0159 \\ 0.3070 & 0.3224 & 0.2509 & 0.1040 & 0.0155 \end{bmatrix} \quad (3.36)$$

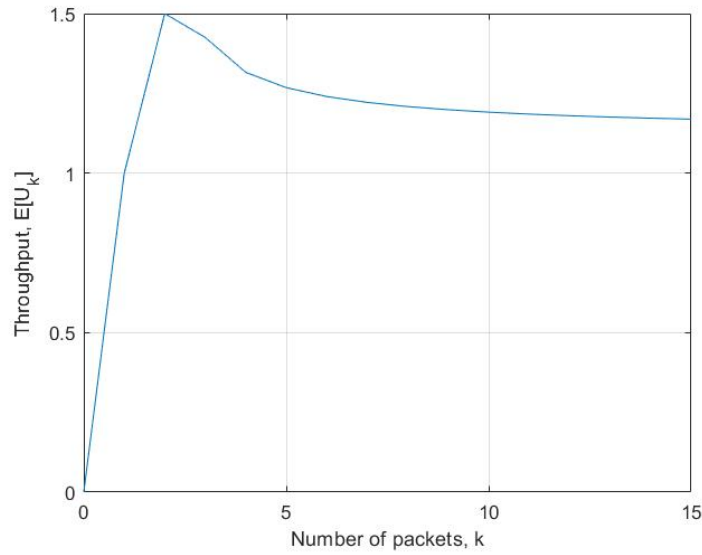


Fig. 3.21. Throughput as a function of the packet arrival rate for $N=4$ power levels

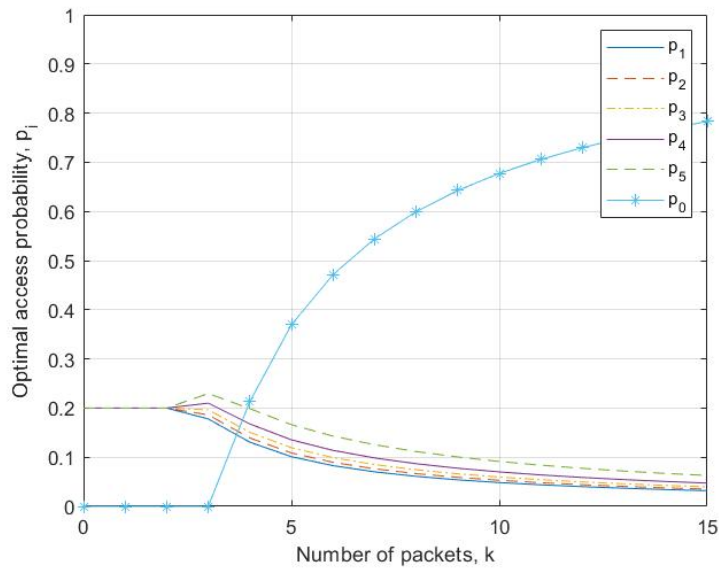


Fig. 3.22. Optimal access probabilities as a function of the number of packets in the system for $N=5$ power levels

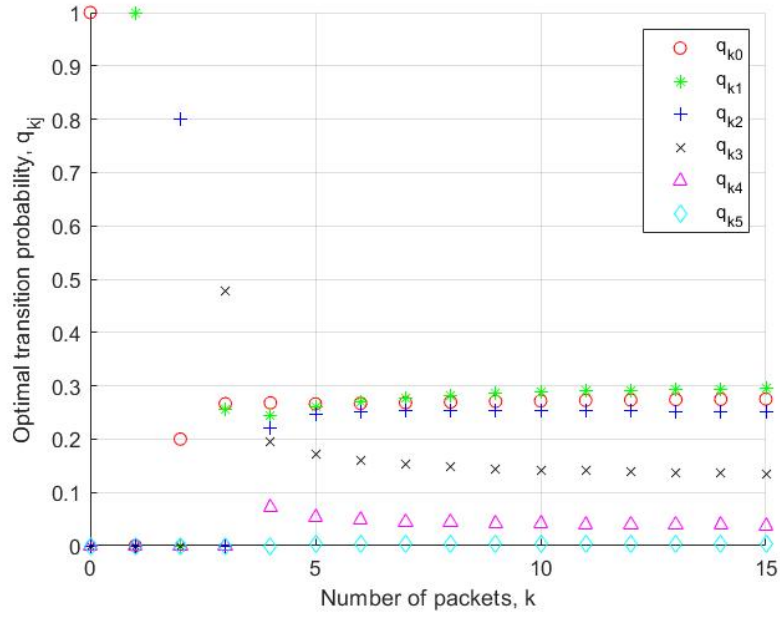


Fig. 3.23. Success probabilities as a function of number of packets for $N=5$ power levels

$$Q_{M+1} = \begin{bmatrix} q_{00} & q_{01} & q_{02} & q_{03} & q_{04} & q_{05} \\ q_{10} & q_{11} & q_{12} & q_{13} & q_{14} & q_{15} \\ q_{20} & q_{21} & q_{22} & q_{23} & q_{24} & q_{25} \\ q_{30} & q_{31} & q_{32} & q_{33} & q_{34} & q_{35} \\ q_{40} & q_{41} & q_{42} & q_{43} & q_{44} & q_{45} \\ q_{50} & q_{51} & q_{52} & q_{53} & q_{54} & q_{55} \\ q_{60} & q_{61} & q_{62} & q_{63} & q_{64} & q_{65} \\ q_{70} & q_{71} & q_{72} & q_{73} & q_{74} & q_{75} \\ q_{80} & q_{81} & q_{82} & q_{83} & q_{84} & q_{85} \\ q_{90} & q_{91} & q_{92} & q_{93} & q_{94} & q_{95} \\ q_{10,0} & q_{10,1} & q_{10,2} & q_{10,3} & q_{10,4} & q_{10,5} \\ q_{11,0} & q_{11,1} & q_{11,2} & q_{11,3} & q_{11,4} & q_{11,5} \\ q_{12,0} & q_{12,1} & q_{12,2} & q_{12,3} & q_{12,4} & q_{12,5} \end{bmatrix} \Rightarrow \begin{bmatrix} 1 & 0 & 0 & 0 & 0 & 0 \\ 0.0001 & 0.9999 & 0 & 0 & 0 & 0 \\ 0.1999 & 0.0001 & 0.7999 & 0 & 0 & 0 \\ 0.2664 & 0.2565 & 0.0001 & 0.4770 & 0 & 0 \\ 0.2680 & 0.2445 & 0.2203 & 0.1959 & 0.0711 & 0 \\ 0.2660 & 0.2597 & 0.2453 & 0.1719 & 0.0534 & 0.0035 \\ 0.2669 & 0.2701 & 0.2511 & 0.1598 & 0.0477 & 0.0040 \\ 0.2683 & 0.2770 & 0.2528 & 0.1527 & 0.0447 & 0.0042 \\ 0.2696 & 0.2818 & 0.2533 & 0.1480 & 0.0429 & 0.0042 \\ 0.2707 & 0.2853 & 0.2532 & 0.1447 & 0.0416 & 0.0042 \\ 0.2717 & 0.2880 & 0.2530 & 0.1421 & 0.0406 & 0.0042 \\ 0.2726 & 0.2901 & 0.2528 & 0.1402 & 0.0399 & 0.0042 \\ 0.2734 & 0.2918 & 0.2525 & 0.1386 & 0.0393 & 0.0042 \end{bmatrix} \quad (3.37)$$

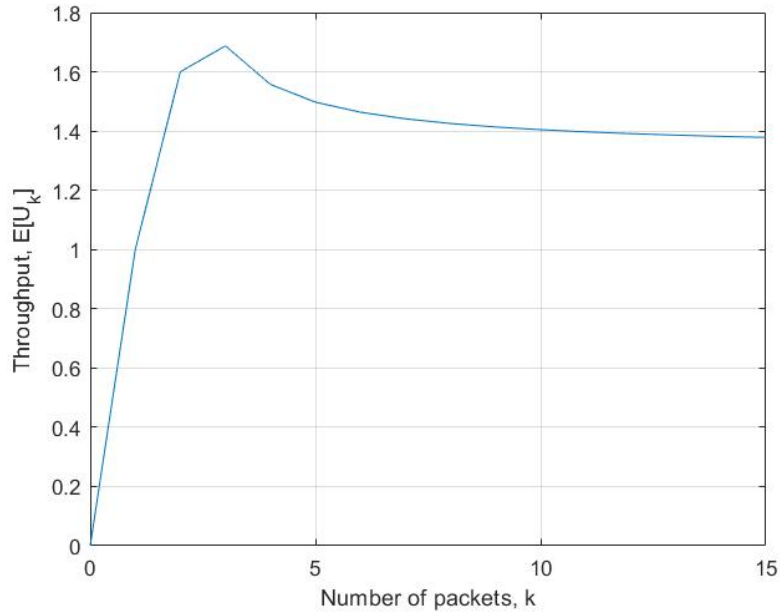


Fig. 3.24. Throughput as a function of the packet arrival rate for $N=5$ power levels

3.3.3 Uniform user access probabilities with non-optional transmit

3.3.3.1 Analysis

In this method, a user chooses power levels uniformly. As in the previous methods, joint probability distribution of the number of packets being transmitted at each power level during a slot is given by the multinomial distribution. Assuming that a user with a packet always transmits during a slot, then we have, $p_i = \frac{1}{N}$, $i = 1..N$. Thus, transmit probabilities are determined from eq. (3.26) with $p_i = \frac{1}{N}$, $i = 1..N$.

For this access method PGF of the probability distribution of the number of packets in the system may be simplified as follows. For this method for the number of packets in the system more than M , probability of transmitting packets successfully drops down to zero, thus, $q_0 = 1$. As a result, eq. (3.13) simplifies to,

$$Q(z) = \frac{\left\{ \sum_{k=0}^M \sum_{j=0}^N z^{k-j} q_{kj} \pi_k - \sum_{k=0}^M z^k \pi_k \right\} A(z)}{1-A(z)}$$

Since $q_0 = 1$, we assume that in a stable system, $\pi_k = 0$ for $k > M$. Thus, we can write down the equations for $\pi = \pi P$ for $0 \leq k \leq M$ and solve these equations together with the normalization condition to determine unknown probabilities.

3.3.3.2 Numerical results and Discussion

Next, we present transition probabilities for uniform access method for systems with number of power levels $N = 2$ to $N = 5$. Fig. 3.25 presents plot of the transition probability as a function of the number of packets in the system for a system with $N = 2$. It can be seen that the probability of successful packet transmission goes to zero with increasing number of packets in the system. Fig. 3.26 plots the throughput of the system as a function of the number of packets in the system. It may be seen that throughput drops to zero with increasing number of packets in the system.

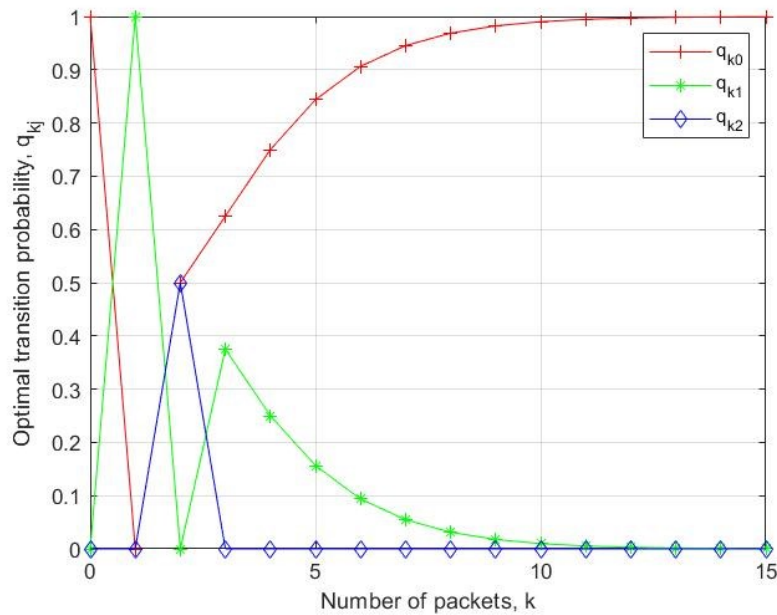


Fig. 3.25. Success probabilities as a function of number of packets for $N=2$ power levels

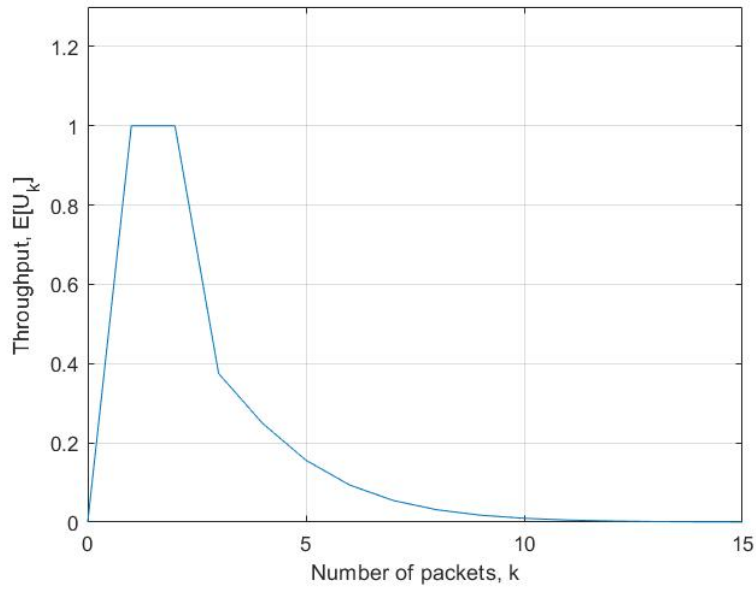


Fig. 3.26. Throughput as a function of the packet arrival rate for $N=2$ power levels

In Fig. 3.27 and Fig. 3.28, we present the transmit probabilities and throughput as a function of the number of packets in the system for $N=3$ power levels. As before, it may be seen that probability of successful packet transmission and therefore throughput goes down to zero for increasing number of the packets in the system.

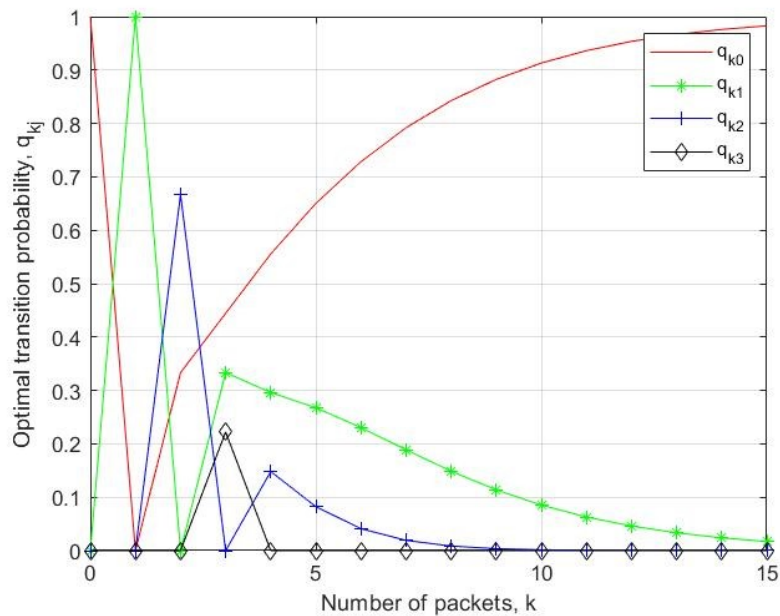


Fig. 3.27. Success probabilities as a function of number of packets for $N=3$ power levels

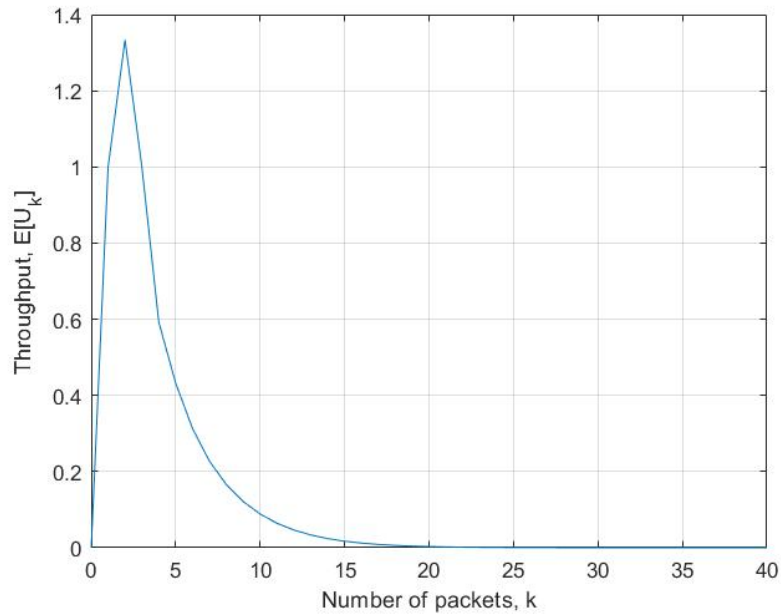


Fig. 3.28. Throughput as a function of the packet arrival rate for $N=3$ power levels

In Fig. 3.29 and Fig. 3.30, we present the transmit probabilities and throughput as a function of the number of packets in the system for $N=4$ power levels. As before, it may be seen that probability of successful packet transmission and therefore throughput goes down to zero for increasing number of the packets in the system.

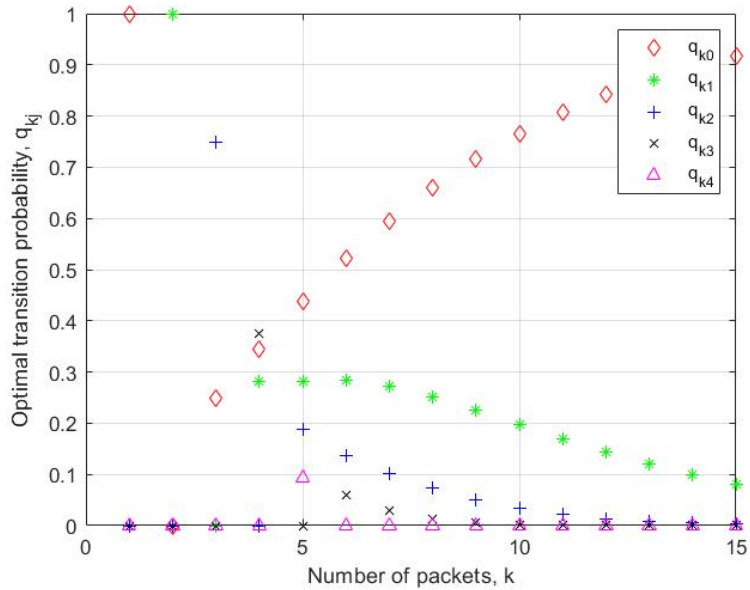


Fig. 3.29. Success probabilities as a function of number of packets for $N=4$ power levels

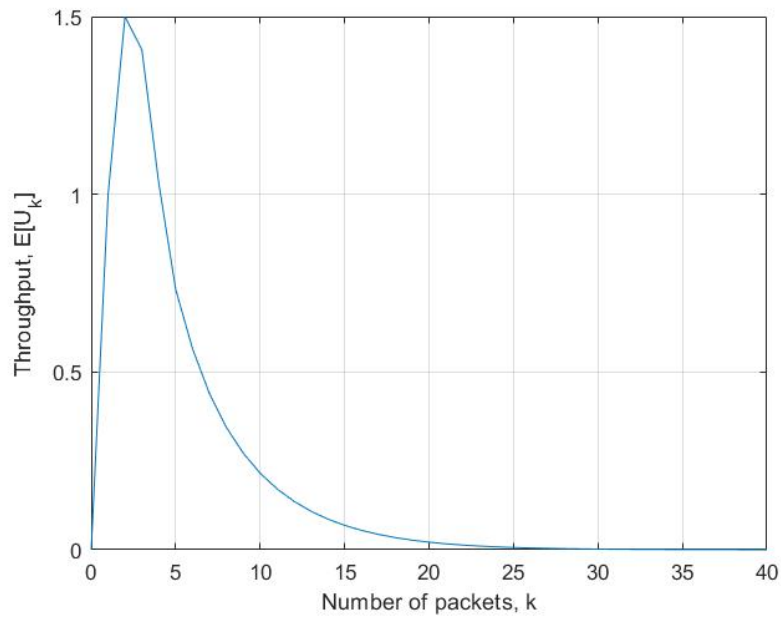


Fig. 3.30. Throughput as a function of the packet arrival rate for $N=4$ power levels

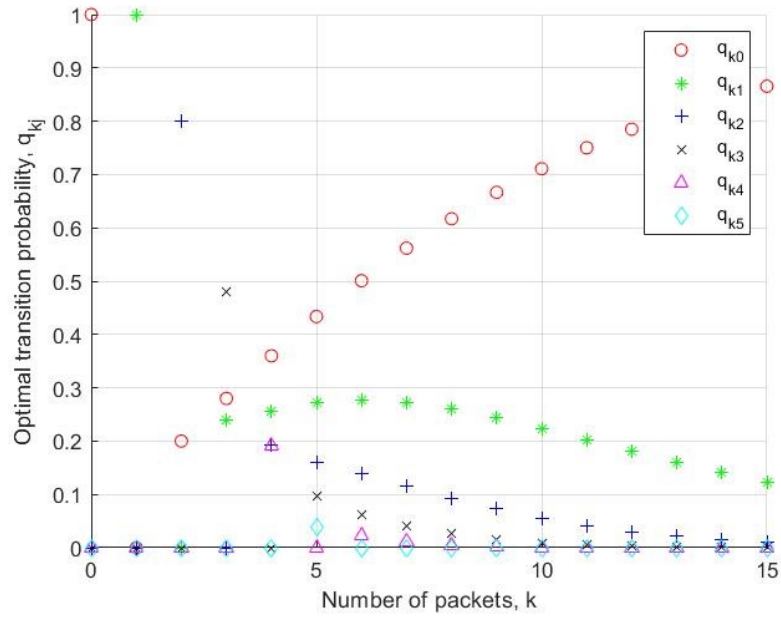


Fig. 3.31. Success probabilities as a function of number of packets for $N=5$ power levels

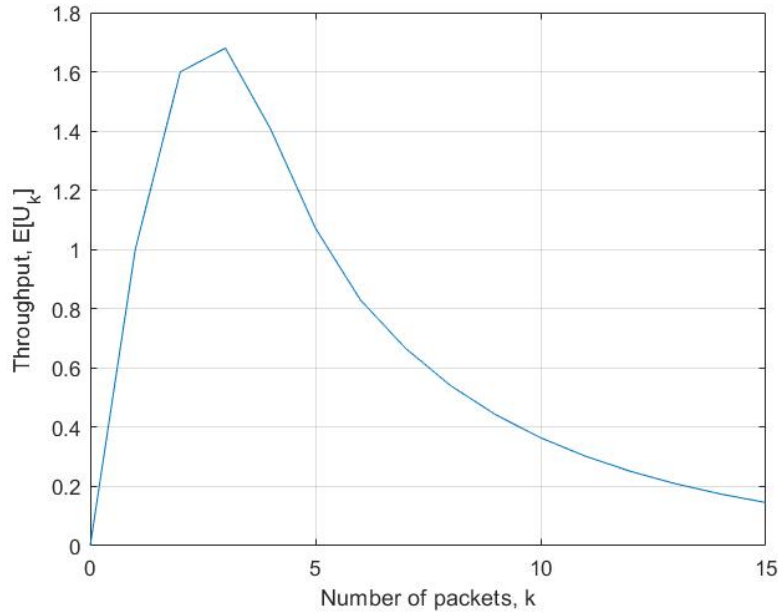


Fig. 3.32. Throughput as a function of the packet arrival rate for $N=5$ power levels

3.3.4 Numerical results for the mean packet delay

Following the determination of the optimal transition probabilities, we determined the $(M+1)$ unknowns in the PGF of the distribution of the number of packets in the queue given by eq. (3.13). First, we determined $N-1$ roots of the denominator of the PGF within the unit circle. Then, we obtained $N-1$ equations through substitution of these roots into the numerator and $M+2-N$ equations from eq. (3.16). Then, we determined $M+1$ unknowns in the PGF through the simultaneous solution of these $M+1$ equations.

Fig. 3.33, Fig. 3.34, and Fig. 3.35 plot the average packet delay as a function of the packet arrival rate for the three user access methods for number of power levels $N=2, 3$ and 4 , respectively. As may be seen, average packet delay increases with increasing arrival rate, however, while $N=2$ system saturates at the arrival rate of $\lambda_{max} \approx 0.1$ packets/slot, $N=3$ system saturates at the arrival rate of $\lambda_{max} \approx 0.35$ packets/slot $N=4$ system saturates at the arrival rate of $\lambda_{max} \approx 0.6$ packets/slot. It may be seen that optimal optional transmit gives the best packet delay performance, then optimal non-optional transmit and uniform access providing the worst performance.

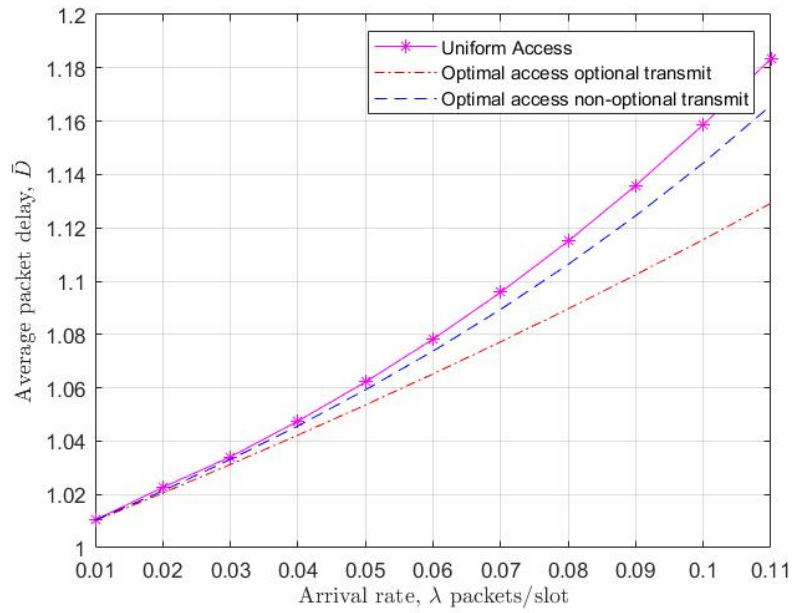


Fig. 3.33. Average packet delay as a function of the packet arrival rate for number of power levels $N=2$

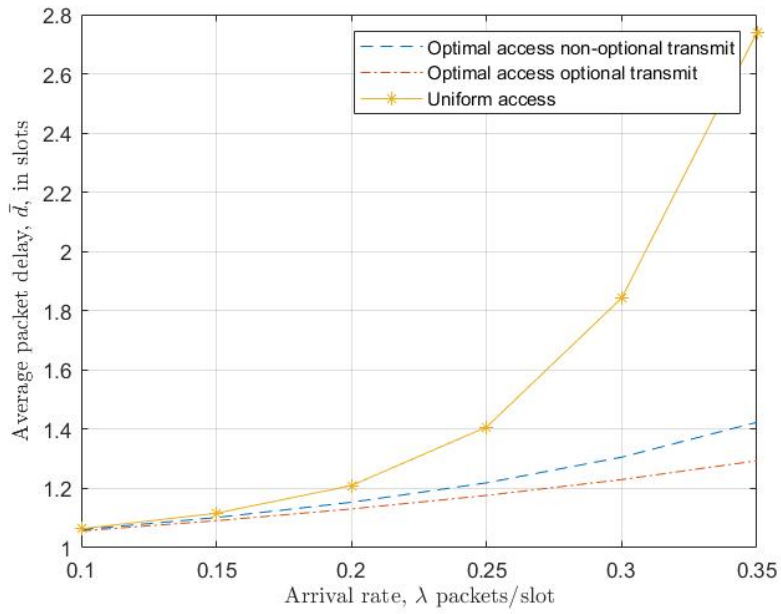


Fig. 3.34. Average packet delay as a function of the packet arrival rate for number of power levels $N=3$

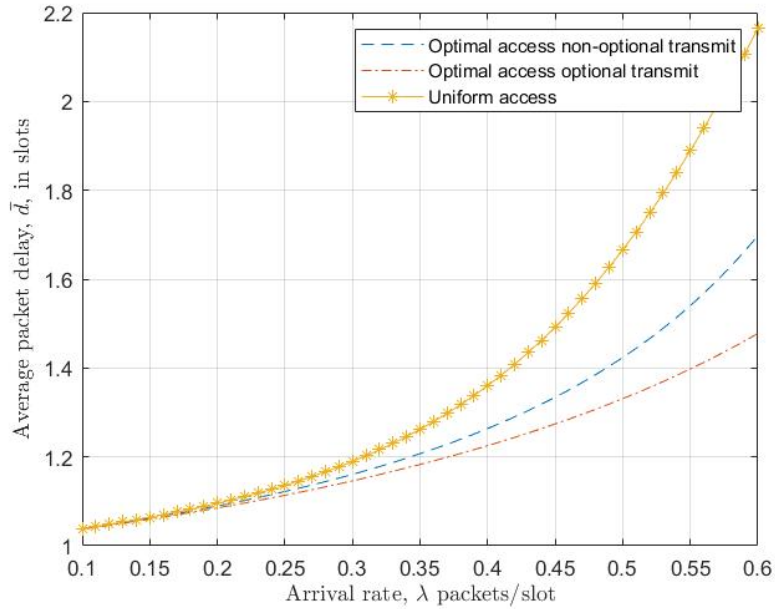


Fig. 3.35. Average packet delay as a function of the packet arrival rate for number of power levels $N=4$

3.4 Conclusion

In this chapter, we proposed a lossless model of a single channel PD-NOMA system. We assumed that each user may have at most single packet waiting to be transmitted at any time. The number of new packet arrivals to the system during a slot is according to a Poisson process. We explicate a mathematical model for the number of packets in the system by imbedding a homogenous Markov chain at the end of the slots. We derived the PGF of the number of packets in the system at the steady-state and determined enough number of equations to solve for the unknowns in the PGF. Then, we obtained the mean packet delay from the PGF of the number of packets in the system through application of the Little's result. Results are demonstrated and compared across three different access methods to the power levels, optimal access with nonoptional transmission, optimal access with optional transmission and uniform access with nonoptional transmission. The numerical results show that optimal access with optional transmission gives the best throughput performance.

Chapter 4

Conclusion and Future Work

In this thesis, we consider a single channel slotted Power Domain NOMA model, with non-uniform power level selection and CSI-aware multiple users. In chapter 2, we developed a throughput optimization model for a system with packet losses and analyzed the performance on the basis of packet transmission probability. Numerical results corroborate that the system serves better with optional transmission of packets with optimal user access probabilities. The maximum throughput is almost N times higher than maximum throughput of slotted Aloha protocol for a system with N power levels and it decreases with increasing arrival rate but it is lower bounded by $N-1$ times maximum throughput of slotted Aloha protocol. The trade-off between NOMA efficiency and power level consumption has also been explicated. Results reveal that the received signal power varies proportionally with traffic load and number of power levels.

In chapter 3, the aforementioned mathematical model is extended to adapt a lossless model and the system is solved for unknown power level access probabilities using PGF and homogeneous Markov chain equations. Average number of successfully transmitted packets is also determined as a function of power level access probabilities and the solution is utilized to obtain the results. Results are demonstrated and compared across three different access methods to the power levels, optimal access with nonoptional transmission, optimal access with optional transmission and uniform access with nonoptional transmission. The numerical results show a better performance in throughput when the user chooses the power levels optionally. Average mean delay is also compared between various methods of user transmission, which corroborates the fact that uniform power level access provides the least numbers in efficiency and performance parameters.

While our thesis brings robust new evidence and evaluation results, the data here is limited to transcriptional level and some assumptions. The knowledge of number of user equipment having packets to transmit is still a concern in a distributed system. Future studies should focus on deployment of an unambiguous model, with a message-aware and user-aware distributed system.

This work should be extended to higher layer model and must consider, the complex parameters like attenuation losses and optimal power allocation. The lossless model should also allow for the possibility of optimal power allocation for critical messages, so that there is minimal latency in high priority deployment such as military applications. With huge amount of data packets and a congestive system, one can collect the data regarding the collision time, duration, and access probability and conveniently extend the model to learn and take measures against collisions preemptively, and facilitate towards a predictive maintenance model.

References

- [1] L. Ericsson, "More than 50 billion connected devices", *White Paper*, 2011.
- [2] K. Zheng, S. Ou, J. Alonso-Zarate, M. Dohler, F. Liu and H. Zhu, "Challenges of massive access in highly dense LTE-advanced networks with machine-to-machine communications," *IEEE Wireless Communications*, vol. 21, no. 3, pp. 12-18, June 2014, doi: [10.1109/MWC.2014.6845044](https://doi.org/10.1109/MWC.2014.6845044).
- [3] L. Dai, B. Wang, Z. Ding, Z. Wang, S. Chen, and L. Hanzo, "A Survey of Non-Orthogonal Multiple Access for 5G," *IEEE Communications Surveys Tutorials*, vol. 20, no. 3, pp. 2294–2323, thirdquarter 2018, doi: [10.1109/COMST.2018.2835558](https://doi.org/10.1109/COMST.2018.2835558).
- [4] T. Manglayev, R. C. Kizilirmak, and Y. H. Kho, "Optimum power allocation for non-orthogonal multiple access (NOMA)," *IEEE 10th International Conference on Application of Information and Communication Technologies (AICT)*, Baku, Azerbaijan, Oct. 2016, pp. 1–4, doi: [10.1109/ICAICT.2016.7991730](https://doi.org/10.1109/ICAICT.2016.7991730).
- [5] T. Manglayev, R. C. Kizilirmak, Y. H. Kho, N. Bazhayev, and I. Lebedev, "NOMA with imperfect SIC implementation," *IEEE EUROCON -17th International Conference on Smart Technologies*, Ohrid, Macedonia, Jul. 2017, pp. 22–25, doi: [10.1109/EUROCON.2017.8011071](https://doi.org/10.1109/EUROCON.2017.8011071).
- [6] A. Benjebbour, Y. Saito, Y. Kishiyama, A. Li, A. Harada, and T. Nakamura, "Concept and practical considerations of non-orthogonal multiple access (NOMA) for future radio access," *International Symposium on Intelligent Signal Processing and Communication Systems*, Nov. 2013, pp. 770–774, doi: [10.1109/ISPACS.2013.6704653](https://doi.org/10.1109/ISPACS.2013.6704653).
- [7] T. Park, G. Lee, and W. Saad, "Message-Aware Uplink Transmit Power Level Partitioning for Non-Orthogonal Multiple Access (NOMA)," *IEEE Global Communications Conference (GLOBECOM)*, Dec. 2018, pp. 1–6, doi: [10.1109/GLOCOM.2018.8647935](https://doi.org/10.1109/GLOCOM.2018.8647935).
- [8] H. Tabassum, E. Hossain and J. Hossain, "Modeling and Analysis of Uplink Non-Orthogonal Multiple Access in Large-Scale Cellular Networks Using Poisson Cluster Processes," *IEEE Transactions on Communications*, vol. 65, no. 8, pp. 3555-3570, Aug. 2017, doi: [10.1109/TCOMM.2017.2699180](https://doi.org/10.1109/TCOMM.2017.2699180).

- [9] J. Choi, "NOMA-Based Random Access With Multichannel ALOHA," *IEEE Journal on Selected Areas in Communications*, vol. 35, no. 12, pp. 2736–2743, Dec. 2017, doi: [10.1109/JSAC.2017.2766778](https://doi.org/10.1109/JSAC.2017.2766778).
- [10] X. Chen, A. Benjebbour, A. Li and A. Harada, "Multi-User Proportional Fair Scheduling for Uplink Non-Orthogonal Multiple Access (NOMA)," *IEEE 79th Vehicular Technology Conference (VTC Spring)*, Seoul, 2014, pp. 1-5, doi: 10.1109/VTCSpring.2014.7022998.
- [11] M. Al-Imari, P. Xiao, M. A. Imran and R. Tafazolli, "Uplink non-orthogonal multiple access for 5G wireless networks," *11th International Symposium on Wireless Communications Systems (ISWCS)*, Barcelona, 2014, pp. 781-785, doi: 10.1109/ISWCS.2014.6933459.
- [12] M. S. Ali, H. Tabassum and E. Hossain, "Dynamic User Clustering and Power Allocation for Uplink and Downlink Non-Orthogonal Multiple Access (NOMA) Systems," *IEEE Access*, vol. 4, pp. 6325-6343, 2016, doi: 10.1109/ACCESS.2016.2604821.
- [13] A. Li, A. Benjebbour, X. Chen, H. Jiang and H. Kayama, "Uplink non-orthogonal multiple access (NOMA) with single-carrier frequency division multiple access (SC-FDMA) for 5G systems", *IEICE Trans. Commun.*, vol. E98.B, no. 8, pp. 1426-1435, 2015.
- [14] J. Choi, "Layered Non-Orthogonal Random Access With SIC and Transmit Diversity for Reliable Transmissions," *IEEE Trans. Commun.*, vol. 66, no. 3, pp. 1262–1272, Mar. 2018.
- [15] Z. Ding, X. Lei, G. K. Karagiannidis, R. Schober, J. Yuan and V. K. Bhargava, "A Survey on Non-Orthogonal Multiple Access for 5G Networks: Research Challenges and Future Trends," *IEEE Journal on Selected Areas in Communications*, vol. 35, no. 10, pp. 2181-2195, Oct. 2017, doi: 10.1109/JSAC.2017.2725519.
- [16] S. M. R. Islam, N. Avazov, O. A. Dobre, and K. Kwak, "Power-Domain Non-Orthogonal Multiple Access (NOMA) in 5G Systems: Potentials and Challenges," *IEEE Communications Surveys Tutorials*, vol. 19, no. 2, pp. 721–742, Secondquarter 2017, doi: [10.1109/COMST.2016.2621116](https://doi.org/10.1109/COMST.2016.2621116).
- [17] T. Cover, "Broadcast channels," *IEEE Transactions on Information Theory*, vol. 18, no. 1, pp. 2-14, January 1972, doi: 10.1109/TIT.1972.1054727.
- [18] S. Vanka, S. Srinivasa, Z. Gong, P. Vizi, K. Stamatiou and M. Haenggi, "Superposition Coding Strategies: Design and Experimental Evaluation," *IEEE Transactions on Wireless*

- Communications, vol. 11, no. 7, pp. 2628-2639, July 2012, doi: 10.1109/TWC.2012.051512.111622.
- [19] W. Dai, H. Wei, J. Zhou and W. Zhou, "An Efficient Message Passing Algorithm for Active User Detection and Channel Estimation in NOMA," IEEE 90th Vehicular Technology Conference (VTC2019-Fall), Honolulu, HI, USA, 2019, pp. 1-6, doi: 10.1109/VTCFall.2019.8891539.
- [20] D. L. Donoho, "Compressed sensing," IEEE Transactions on Information Theory, vol. 52, no. 4, pp. 1289-1306, April 2006, doi: 10.1109/TIT.2006.871582.
- [21] T. S. Rappaport, Wireless Communications: Principles and Practice, New York, NY, USA:Prentice-Hall, 1998.
- [22] H. Lee, S. Kim and J. Lim, "Multiuser Superposition Transmission (MUST) for LTE-A systems," 2016 IEEE International Conference on Communications (ICC), Kuala Lumpur, pp. 1-6, doi: 10.1109/ICC.2016.7510909.
- [23] L. Zhang et al., "Layered-division-multiplexing: Theory and practice", IEEE Trans. Broadcast., vol. 62, no. 1, pp. 216-232, Mar. 2016.
- [24] Z. Ding, R. Schober, P. Fan, and H. V. Poor, "Simple Semi-Grant-Free Transmission Strategies Assisted by Non-Orthogonal Multiple Access," *IEEE Transactions on Communications*, vol. 67, no. 6, pp. 4464–4478, Jun. 2019, doi: [10.1109/TCOMM.2019.2903443](https://doi.org/10.1109/TCOMM.2019.2903443).
- [25] A. Bayesteh, E. Yi, H. Nikopour and H. Baligh, "Blind detection of SCMA for uplink grant-free multiple-access," 11th International Symposium on Wireless Communications Systems (ISWCS), Barcelona, 2014, pp. 853-857, doi: 10.1109/ISWCS.2014.6933472.
- [26] J. Choi, "Re-Transmission Diversity Multiple Access Based on SIC and HARQ-IR," IEEE Trans. Commun., vol. 64, no. 11, pp. 4695–4705, Nov. 2016.
- [27] G. Liva, "Graph-Based Analysis and Optimization of Contention Resolution Diversity Slotted ALOHA," IEEE Transactions on Communications, vol. 59, no. 2, pp. 477-487, February 2011, doi: 10.1109/TCOMM.2010.120710.100054.
- [28] E. Paolini, G. Liva and M. Chiani, "Coded Slotted ALOHA: A Graph-Based Method for Uncoordinated Multiple Access," IEEE Transactions on Information Theory, vol. 61, no. 12, pp. 6815-6832, Dec. 2015, doi: 10.1109/TIT.2015.2492579.

- [29] E. Paolini, C. Stefanovic, G. Liva and P. Popovski, "Coded random access: applying codes on graphs to design random access protocols," *IEEE Communications Magazine*, vol. 53, no. 6, pp. 144-150, June 2015, doi: 10.1109/MCOM.2015.7120031.
- [30] Y. Liang, X. Li, J. Zhang, and Z. Ding, "Non-Orthogonal Random Access for 5G Networks," *IEEE Transactions on Wireless Communications*, vol. 16, no. 7, pp. 4817-4831, July 2017, doi: 10.1109/TWC.2017.2703168.
- [31] N. Zhang, J. Wang, G. Kang and Y. Liu, "Uplink Nonorthogonal Multiple Access in 5G Systems," *IEEE Communications Letters*, vol. 20, no. 3, pp. 458-461, March 2016, doi: 10.1109/LCOMM.2016.2521374.
- [32] J.F. Hayes, & T.V.G. Babu, *Modeling and Analysis of Telecommunications Networks*. John Wiley & Sons, (2004).
- [33] K. Selvam and K. Kumar, "Energy and Spectrum Efficiency Trade-off of Non-Orthogonal Multiple Access (NOMA) over OFDMA for Machine-to-Machine Communication," *Fifth International Conference on Science Technology Engineering and Mathematics (ICONSTEM)*, Mar. 2019, vol. 1, pp. 523–528, doi: [10.1109/ICONSTEM.2019.8918884](https://doi.org/10.1109/ICONSTEM.2019.8918884).
- [34] G. Liva, "Graph-Based Analysis and Optimization of Contention Resolution Diversity Slotted ALOHA," *IEEE Transactions on Communications*, vol. 59, no. 2, pp. 477-487, February 2011, doi: 10.1109/TCOMM.2010.120710.100054.
- [35] E. Casini, R. De Gaudenzi and O. Del Rio Herrero, "Contention Resolution Diversity Slotted ALOHA (CRDSA): An Enhanced Random Access Scheme for Satellite Access Packet Networks," *IEEE Transactions on Wireless Communications*, vol. 6, no. 4, pp. 1408-1419, April 2007, doi: 10.1109/TWC.2007.348337.